



# The climate of Europe during the Holocene: a gridded pollen-based reconstruction and its multi-proxy evaluation



A. Mauri <sup>1</sup>, B.A.S. Davis <sup>\*.2</sup>, P.M. Collins, J.O. Kaplan <sup>2</sup>

ARVE Group, Institute of Environmental Engineering, Ecole Polytechnique Fédérale de Lausanne, CH-1015, Switzerland

## ARTICLE INFO

### Article history:

Received 17 July 2014

Received in revised form

13 January 2015

Accepted 14 January 2015

Available online 16 February 2015

### Keywords:

Pollen-climate

Multi-proxy comparison

Gridded reconstruction

Holocene

Europe

## ABSTRACT

We present a new gridded climate reconstruction for Europe for the last 12,000 years based on pollen data. The reconstruction is an update of Davis et al. (2003) using the same methodology, but with a greatly expanded fossil and surface-sample dataset and more rigorous quality-control. The modern pollen dataset has been increased by more than 80%, and the fossil pollen dataset by more than 50%, representing almost 60,000 individual pollen samples. The climate parameters reconstructed include summer/winter and annual temperatures and precipitation, as well as a measure of moisture balance, and growing degree-days above 5 °C. Confidence limits were established for the reconstruction based on transfer function and interpolation uncertainties. The reconstruction takes account of post-glacial isostatic readjustment which resulted in a potential warming bias of up to +1–2 °C for parts of Fennoscandia in the early Holocene, as well as changes in palaeogeography resulting from decaying ice sheets and rising post-glacial sea-levels. This new dataset has been evaluated against previously published independent quantitative climate reconstructions from a variety of archives on a site-by-site basis across Europe. The results of this comparison are generally very good; only chironomid-based reconstructions showed substantial differences with our values. Our reconstruction is available for download as gridded maps throughout the Holocene on a 1000-year time-step. The gridded format makes our reconstructions suitable for comparison with climate model output and for other applications such as vegetation and land-use modelling. Our new climate reconstruction suggests that warming in Europe during the mid-Holocene was greater in winter than in summer, an apparent paradox that is not consistent with current climate model simulations and traditional interpretations of Milankovitch theory.

© 2015 Elsevier Ltd. All rights reserved.

## 1. Introduction

While large-scale, gridded, quantitative paleoclimate reconstructions have existed for some time, these tended to be limited to individual timeslices or time windows, e.g., the mid-Holocene (6 ka), LGM (21 ka) or the last millennium. As advances continue to be made in computing power, multi-millennial transient experiments with global climate models (GCMs) are being increasingly undertaken (Renssen et al., 2005, 2009, 2012; Lorenz et al., 2006; Lohmann and Lorenz, 2007; Fischer and Jungclaus,

2011; Liu et al., 2011; Singarayer et al., 2011). Evaluation of these GCM experiments therefore requires quantitative climate reconstructions that are continuous over long time periods and large spatial scales (Bartlein et al., 2010).

Previous evaluation of paleoclimate model simulations with proxy based reconstructions has shown that GCMs continue to have difficulty simulating many key aspects of Holocene climate (Braconnot et al., 2012; Hargreaves et al., 2013), including the climate of Europe (Masson et al., 1999; Bonfils et al., 2004; Brewer et al., 2007b; Mauri et al., 2014), and particularly the climate changes indicated by reconstructions for Southern Europe (Davis and Brewer, 2009). Transient-model simulations have also shown that these mid-Holocene data-model discrepancies reflect systematic differences between models and climate reconstructions throughout much of the Holocene (Fischer and Jungclaus, 2011).

These data-model discrepancies have been based primarily on palaeoclimate reconstructions based on pollen data, which

\* Corresponding author.

E-mail address: [basil.davis@unil.ch](mailto:basil.davis@unil.ch) (B.A.S. Davis).

<sup>1</sup> Now at the European Commission Joint Research Centre, Institute for Environment and Sustainability, Via E. Fermi 2749, I-21027 Ispra (VA), Italy.

<sup>2</sup> Now at the ARVE Group, Institute of Earth Surface Dynamics, University of Lausanne, CH-1015, Switzerland.

represents the most widely available proxy at continental-scales for the entire Holocene time period. Inevitably, questions have been raised about the reliability of these reconstructions, particularly since not all sites or types of paleoclimate proxies show the same results (Renssen et al., 2012). This in part reflects the difficulty of comparing studies that assimilate many hundreds of sites to extract the underlying regional response (relevant to the low resolution grid-box scale of climate models), with individual sites whose records can reflect a very localised climate response (Davis et al., 2003). It also highlights problems with poor site coverage in some regions of Europe in earlier studies, as well as the quality of the training sets of modern pollen surface samples (Davis et al., 2013).

Demand for gridded palaeoclimate data for the Holocene has also come from other scientific fields beyond climate modelling. This includes studies of the post-glacial development of European vegetation, where attempts to use palaeoclimate data from climate models to simulate the past distribution of vegetation have been problematic (Giesecke et al., 2007, 2008). This potentially reflects the same problems with the ability of models to simulate Holocene climate mentioned earlier, and has increased interest in using reconstructed palaeoclimate data (in this case, pollen-based) to drive the vegetation models, an approach that appears to have met with more success (Slatre et al., 2013). There has also been a growing interest in investigating the potential role of climate in shaping the development of human civilisation in the European region during the Holocene. For instance, climate amelioration has been highlighted as a possible reason for the timing of the spread of early agriculture into north-west Europe (Bonsall et al., 2001). Recent developments in the modelling of early civilisations have made use of palaeoclimate data to model the spread of the Neolithic in Europe using agent-based models (Lemmen and Wirtz, 2012). This work has mainly used records from a few individual sites (including North Atlantic SST's) as a proxy for European scale changes, and has not used spatially explicit gridded datasets. Such data is required however to facilitate the incorporation of palaeoclimate data into models of Holocene anthropogenic land cover change, which will represent the next step in the use of such modelling which at present generally use a fixed modern climate in generating Holocene-long scenarios (e.g., Kaplan et al., 2009).

Previous attempts to reconstruct the Holocene climate of Europe in a quantitative and spatially extensive way have mainly focused on the mid-Holocene (Huntley and Prentice, 1988; Cheddadi et al., 1997; Wu et al., 2007; Brewer et al., 2007b; Mauri et al., 2014), although some have also used widely spaced timeslices such as every 3000 years (Guio et al., 1993). These studies have all used pollen data, which is by far the most widely available quantitative climate proxy for the Holocene period. The only previous attempt to investigate Holocene climate at the European scale continuously throughout the last 12,000 years is that of Davis et al. (2003). This study also differed from previous studies in using a 4-D interpolation method to 'focus' the reconstruction onto a regular time-step, rather than relying on the time-window approach that has been employed in almost all previous studies. For instance, most mid-Holocene studies have used a time window of 6000 years BP  $\pm$  500 years, either taking the average of all the samples falling within this window, or the closest to the target time. This method leads to temporal 'blurring' with samples being compared that are up to 1000 years distant from each other and 500 years distant from the target time. The method of Davis et al. (2003) used a distance weighting to assign greater weight to samples closer to the target time in the same way that distance weighting assigns greater weight to samples closer in distance. The spatial interpolation also takes account of the different altitudes of the samples and grid points, combining interpolation across 3-

dimensional space with the 4th dimension, time, to create a regular spatial and temporal grid.

In this paper we present an updated version of the Davis et al. (2003) study using the same modern analogue pollen-climate calibration technique based on PFT (plant functional type) scores and the same 4D interpolation technique to produce gridded paleoclimate maps. In this new analysis we make use of recent improvements in data quality and availability to greatly increase the number of samples and sites analysed, including the surface sample training set. Data has come from the European Pollen Database (EPD), together with additional fossil data from the PANGAEA archive and other data sources (Collins et al., 2012). The modern pollen calibration training set has been increased by 81% compared to Davis et al. (2003), while the fossil pollen dataset has been improved by more than 50% representing almost 60,000 individual pollen samples in the fossil dataset. As well as this very large increase in primary data, we have also incorporated a number of other innovations not included in the Davis et al. (2003) analysis, including the following:

- 1) The number of climate parameters has been extended to include growing degree-days above 5 °C (GDD5), annual and seasonal precipitation, and a measure of moisture balance (P-E). Davis et al. (2003) presented seasonal temperatures based on the warmest or coldest month, but here we use seasonal averages (DJF, JJA), which are more widely used in climate modelling. Similarly, we present seasonally averaged precipitation for the same reason, and also because it is a minimum requirement as input for dynamic vegetation models.
- 2) A significant new advance in our analysis has been the incorporation of palaeogeographic changes that occurred in Europe over the Holocene, including elevation and sea level changes. Melting of the Fennoscandian ice sheet at the end of the Pleistocene and early Holocene resulted in isostatic rebound of up to 300 m in some regions. Sites in these areas today were potentially therefore much closer to sea level at the start of the Holocene, which could lead to warmer temperatures (+1–2 °C) even if no large-scale climate change occurred. As a result of these residual LGM ice sheets, sea levels were also lower during the early Holocene (Carlson, 2011). We have included both eustatic and isostatic effects in our analysis, allowing us to show many features of the early Holocene European landscape that have since disappeared, such as the early expanded Baltic sea/lake and the ancient Doggerland that now lies beneath the North Sea (Gaffney et al., 2009).
- 3) Our reconstruction includes a series of quality control checks and full-error accounting of the transfer function (Bartlein et al., 2010) and interpolation errors, which allow us to establish and map confidence limits for our climate reconstruction.
- 4) We have evaluated our reconstruction against other independent reconstructions of Holocene climate based on both pollen and other proxies. This has been possible using the interpolation methodology to directly compare records on a site-by-site basis within the European study region.

## 2. Methods

### 2.1. Modern and fossil pollen dataset

The surface samples used in our analysis were obtained from the European Modern Pollen Database (EMPD) project (Davis et al., 2013). This dataset includes over 4700 surface pollen samples provided by over 40 individual authors and research groups. It has

undergone rigorous quality control in terms of taxonomy harmonisation, provenance, metadata documentation and removal of duplicates, and only includes primary data representing the full sample assemblage (Davis et al., 2013). We further performed an additional quality check on the georeferencing of each modern pollen sample using a high-resolution digital elevation model (DEM). Poor georeferencing affects the climate reconstruction through the assignment of spurious modern climate to a modern pollen spectrum; we excluded samples from our analysis where the difference between the recorded elevation of the sampling site was different from the DEM elevation for that longitude and latitude by more than 250 m. This additional filter resulted in the exclusion of ~11% of the surface samples from the dataset. This nevertheless left a total of 4287 samples widely distributed across Europe west of the Urals, representing an 81% improvement in the size of the training set used by Davis et al. (2003). The modern climate for each pollen surface sample site was determined from the 1-km high-resolution gridded climatology of Hijmans et al. (2005) which improves on the 0.5° resolution grid of Leemans and Cramer (1991) used in many previous studies.

The fossil pollen dataset was compiled from the European Pollen Database (EPD), together with additional data from the PANGAEA archive (<http://www.pangaea.de>) and other sources (Collins et al., 2012). We assimilated all taxon names to conform to EPD standards, and ensure compatibility between modern and fossil datasets. Overall, the fossil pollen database has been expanded by more than 50% relative to the Davis et al. (2003) dataset, comprising a total number of 879 selected pollen sites representing nearly 60,000 pollen counts. Spatial coverage of fossil sites has been improved across Europe in comparison with Davis et al. (2003), but particularly in Southern and Northern Europe (Fig. 1). Some sites have also been excluded that were part of the Davis et al. (2003) analysis, due to more rigorous selection criteria, particularly regarding dating control. Chronology is based on individually calibrated age–depth models and only sites with a minimum of at least two independent dates (for instance, radiocarbon dates) were included with an average of 6 control points per site excluding finely dated laminated sequences which had considerably more.

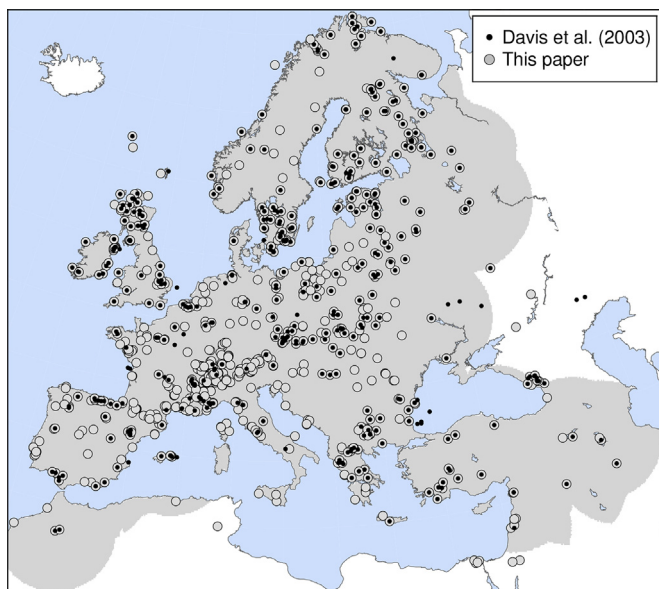


**Fig. 1.** Spatial distribution of pollen sites (open circles) used to reconstruct the climate for the Holocene. Interpolated climate values were limited to a distance of 500 km from the pollen site location (shaded area). The number of sites analysed represents 53% increase compared to Davis et al. (2003) (filled circles).

## 2.2. Pollen climate reconstruction

Palaeoclimate was reconstructed for each pollen sample with the R package 'Rioja' (Juggins, 2012) using a Plant Functional Type (PFT) Modern Analogue Technique (MAT) as detailed in Davis et al. (2003), and based on the PFT definitions of Peyron et al. (1998). We decided to use MAT because it is considered to be the most suitable method for large-scale climate reconstructions, especially when as in this case the training set encompasses a wide range of vegetation and climate zones (Brewer et al., 2007a; Birks et al., 2010; Juggins and Birks, 2011). The reason for using PFT scores is explained more fully in Davis et al. (2003), but in summary it helps reduce the impact of non-climatic disturbance (including anthropogenic disturbance) on the pollen record, as well as reducing problems associated with finding modern-analogues for some fossil taxa assemblages. We reconstructed a range of well-established climate parameters used in pollen-climate analysis, including mean summer (JJA), winter (DJF) and annual temperature and precipitation, mean annual GDD5 (growing degree days over 5 °C) and mean annual P–E (precipitation minus evaporation) (Bartlein et al., 2010). Seasonal precipitation is a relatively new parameter but has nevertheless been reconstructed from pollen data in many studies in Eurasia (Penalba et al., 1997; Finsinger et al., 2007; Wu et al., 2007; Kotthoff et al., 2008; Nakagawa et al., 2008; Combourieu Nebout et al., 2009; Peyron et al., 2011).

An evaluation of the climate reconstruction method based on n-fold-leave-one-out cross validation is shown in Table 1. This evaluation works by splitting the modern training set into random subsets. As each subset is removed from the dataset in turn, the remaining modern samples are used to generate reconstruction models that are then applied to the omitted samples. The process is repeated for each subset to give a leave-one-out climate estimate for each modern sample. This data-splitting procedure is repeated 5 or 10 times, each with random partitions of the modern data providing a more reliable estimate of the model performance than is provided by simple leave-one-out cross-validation, especially using MAT where the effect of spatial autocorrelation can otherwise cause uncertainty to be under-estimated (Barrows and Juggins, 2005). The results show that reconstructed values closely match observed values, with winter precipitation representing the most difficult parameter to reconstruct at the European scale.

## 2.3. Gridding procedure and uncertainties

Palaeoclimate reconstructions for each dated pollen sample were then interpolated in four-dimensions onto a uniform spatial grid and time-step using a four-dimensional Thin Plate Spline (4D-TPS) interpolation method from the R package 'fields' (Furrer et al., 2010). The interpolation spline model can be applied at any

**Table 1**

Observed and pollen-inferred modern climate values based on n-fold-leave-one-out cross-validation. For each climate variable we report the coefficient of determination ( $r^2$ ), the root mean square error (RMSE) and the actual error. Temperatures and GDD5 are expressed in °C. Precipitation and moisture balance (P–E) are expressed in mm/month.

Climate parameter	Correlation ( $r^2$ )	RMSE	Error
Winter (DJF) temperature	0.85	2.78	±1.67 (°C)
Winter (DJF) precipitation	0.49	28.8	±5.37 (mm)
Summer (JJA) temperature	0.71	2.59	±1.61 (°C)
Summer (JJA) precipitation	0.78	17.6	±4.20 (mm)
Annual temperature	0.81	2.42	±1.56 (°C)
Annual precipitation	0.61	7.5	±6.9 (mm)
Growing degree days (GDD5)	0.73	570.4	±23.9 (°C)
Precipitation–evaporation	0.59	7.15	±6.77 (mm)

temporal and spatial resolution, but is presented here at a 1° spatial resolution and 1000 year time-step. The method interpolates through time as well as 3-dimensional space such that the samples closer to the target time and grid point position (both horizontal and vertical) are given a greater weight. For computational reasons only samples within a ±500 year time window around the target time are considered since the weighting decays rapidly with time and samples beyond ±250 years have very little weight. The method therefore focuses the reconstruction onto the target time, and avoids the temporal blurring associated with other methods such as the 'time-window' approach which use an average of all the samples within a time window, such as 6000 ± 500 years BP (Cheddadi et al., 1997; Sawada et al., 2004).

We were able to assign confidence limits to our climate reconstruction (Figs. S5–S8) by combining the uncertainties calculated by the transfer function with those of the interpolation. This was achieved by first calculating the standard error of all of the samples lying within each 1° grid box (Bartlein et al., 2010). To this was then added the standard error generated by the interpolation process (Furrer et al., 2010). The interpolation error generally increases with distance from any sample location, so we also imposed a conservative 500 km limit on the interpolation from the nearest data point, as used by Davis et al. (2003). In addition, we also removed from the dataset samples that had a particularly high uncertainty and therefore could not provide reliable climatic information. These were usually samples that had low taxonomic diversity and were dominated by taxa that are climatic generalists, such as *Pinus* and Poaceae. The threshold varied according to the climatic parameter, but around 3–5% of the total number of samples for each parameter were excluded in this way.

Davis et al. (2003) calculated Holocene climate anomalies relative to late preindustrial time, centred approximately around 100 BP (1850 AD), and we adopt the same convention here. This differs from most comparable palaeoclimate reconstructions that use the 'core top' or modern climate as the baseline for calculating anomalies, such as Bartlein et al. (2010). It has been argued (Sundqvist et al., 2010; Zhang et al., 2010) that the use of a preindustrial baseline for calculating climate anomalies is more appropriate for data-model comparisons, because almost all model simulations are presented as anomalies compared to a preindustrial control run and not modern climate. Given the level of recent climate warming, anomalies based on modern climate would under-estimate past warming compared to models, and over-estimate past cooling. In establishing the baseline climate using the 4D-TPS method, Davis et al. (2003) also note the problem of progressively fewer samples being available to guide the interpolation on the 'future' side of the target time slice in the last 500 years of the time series. For instance, at the 100 BP time-slice, the interpolation uses samples ±500 years either side, but whilst there are samples back to 600 BP, there are no samples in our dataset that extend beyond –60 BP (AD 2010). This could potentially cause time-biasing in the interpolation. To compensate for this, we applied the concept of 'zero-padding' (Castiglioni, 2005) at each core site whereby we artificially extended the record at each core site into the future to –400 BP using samples with the same zero anomaly value.

Chronological control is based on individually fitted age–depth models for each site using over 3500 calibrated radiocarbon dates and over 2400 other independent absolute dates based on varves, tephra and other radiometric dating methods (Davis et al., 2003; Giesecke et al., 2014). Average dating uncertainties range from ±70 years in the late Holocene to ±250 years in the early Holocene (Fig. S9). Maps are presented at 1000 year intervals and time-series at 500 year intervals, which are both well within these uncertainties. Note however that the level of uncertainty means that

sub-millennial scale events are not clearly resolved, and that the 12k map will include both elements of the Younger Dryas and early Holocene.

#### 2.4. Isostatic correction and sea level changes

A significant new advance in our analysis has been the incorporation of isostatic readjustment, ice sheet extent and sea level changes. Maps of the early Holocene ice sheets in Northern Europe were provided by the Digital ATlas of the Eurasian Deglaciation (DATED2) Project (Gyllencreutz et al., 2007). These are based on published records of ice marginal deposits and interpreted isochrones, and show that late Quaternary ice sheets were still very extensive over Scandinavia at the start of the Holocene but had retreated considerably by 10 ka and disappeared almost entirely by 9 ka. The Fennoscandian ice sheet was several km thick at the Last Glacial Maximum causing the Earth's crust in the region to be substantially depressed. Later, as the ice sheet melted and the over bearing weight was removed, the ground beneath started to rise and continues to do so to this day. In regions close to the centre of the former ice sheet around the present northern Gulf of Bothnia post-glacial uplift has been over 300 m, of which over 150 m has occurred in the last 12,000 years. This isostatic rebound affects many pollen sites in Fennoscandia and has important implications for the interpretation of reconstructed paleoclimate at these sites, because a site today could have been more than 150 m closer to sea level at the start of the Holocene. As a result of the simple lapse rate relationship between climate and elevation, a site that was isostatically depressed in the early Holocene would have had a warmer climate compared to present even if no change in large-scale climate had occurred. In order to calculate the climatic effect of this change in altitude, we used the topographic anomalies generated by the ICE-5G glacial isostasy model (VM2 L90; Peltier, 2004, 2009). The ICE-5G model output includes global ice sheet coverage, ice thickness and paleotopography at a 10 arc-minute spatial resolution at 500-year intervals for the last 21,000 years. To correct for the effect that isostatic adjustment had on reconstructed paleoclimate over the Holocene, we created an artificial "elevation-corrected" baseline climate at each 500-year timestep by interpolating baseline modern climate on the paleotopography, implicitly using the present-day topographic lapse rate to calculate the climate on an altered topographic surface. We then generated climate anomalies for each time slice by subtracting the reconstructed paleoclimate from this adjusted baseline climate.

As an example, we show in Fig. 2 the effect of isostatic rebound on winter temperature anomalies throughout the Holocene in Fennoscandia. Isostatic adjustment mainly affects those areas covered with ice (or under water) in the very earliest Holocene, so the effects are less obvious until around 10 ka, when the melting of the ice sheet was almost complete and land started to emerge from the palaeo-Baltic. Temperature anomalies are shown to be greatest in those areas that have since rebounded the most, reaching almost 1.5 °C in areas around the North Western coast of the Gulf of Bothnia, e.g., as shown on the map of 9 ka. The warming effect starts decreasing at 8 ka and by 5 ka the effects of changing altitude become minimal. However, even at the mid-Holocene (6 ka), some 4000 years after deglaciation, the relative warming effect remains in the order of 0.5–0.8 °C in some areas of Northern Europe.

Sea level was calculated by applying a flood-fill algorithm to a global topography and bathymetry dataset (ETOPO1; Amante and Eakins, 2009) adjusted by the ICE-5G paleotopographic anomalies described previously, which was also used to establish the relative sea level for the global oceans. For the Black and Caspian seas we additionally used local sea level curves for the Holocene (Bruckner et al., 2010; Kakroodi et al., 2012). Our palaeogeographic analysis

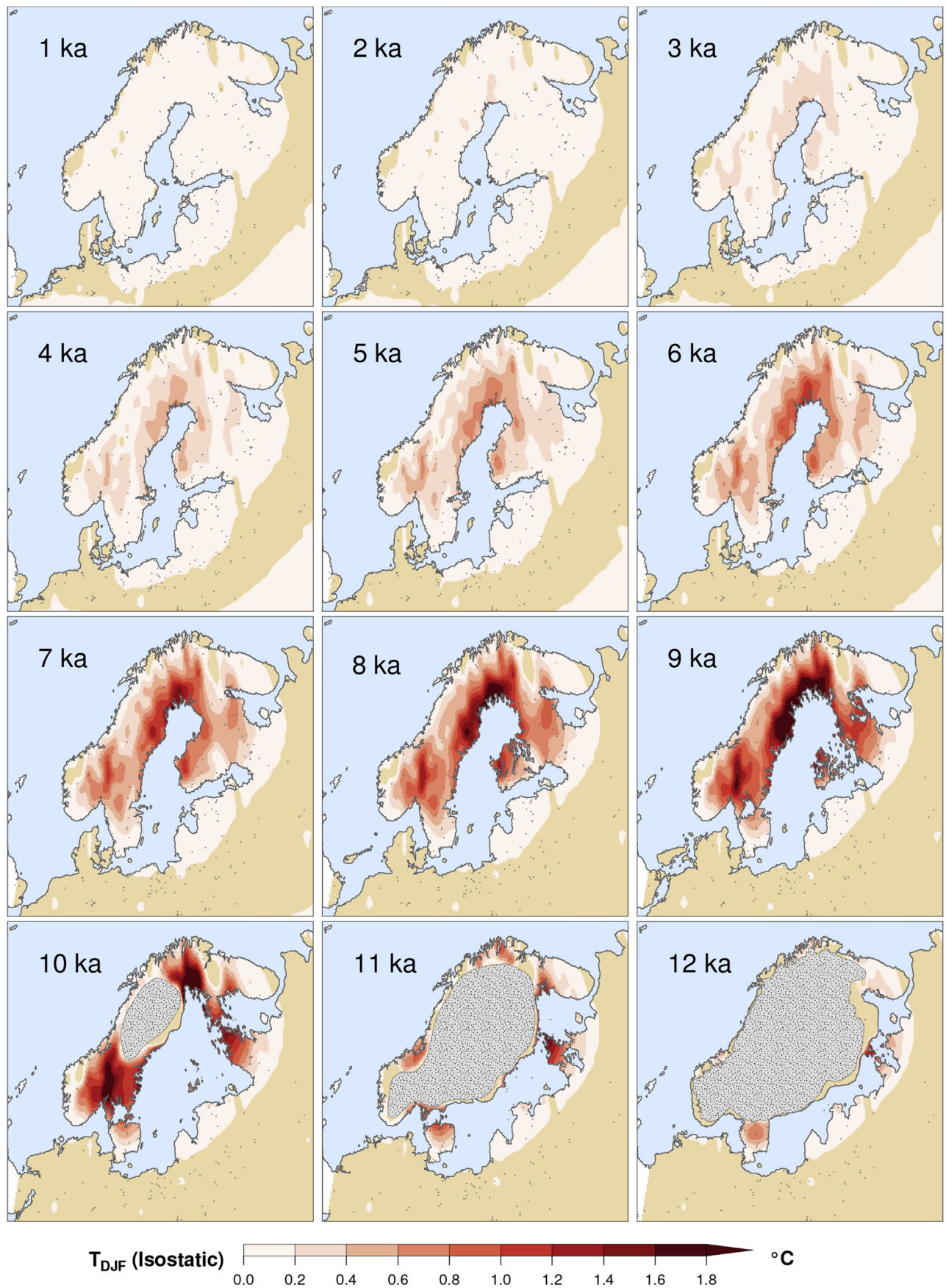


**Fig. 2.** The relative warming effect resulting from post-glacial isostatic rebound, shown here for winter temperature anomalies (units  $^{\circ}\text{C}$ ). The warming is due to sites being at lower altitude in the early–mid Holocene when the land was still heavily depressed from the weight of LGM ice over Scandinavia. The greatest warming anomalies occur in the early Holocene but they persist at significant levels until the mid-Holocene. Changes in coastline and ice sheet extent (Gyllencreutz et al., 2007) are also shown.

shows many important features of the early Holocene European landscape that have since disappeared (Fig. 3), such as the early expanded Baltic sea/lake, the ancient Doggerland that now lies beneath the North Sea (Gaffney et al., 2009) and formerly subaerial lands around the Adriatic, Black Sea, Caspian Sea and Southern Mediterranean coast. Note however that the apparent link between the Baltic and Barents Sea across northwestern Russia is unlikely to have occurred, and instead reflects the limitations of the temporal and spatial resolution of the palaeotopography estimates in areas of low relief.

### 3. Results

#### 3.1. Summer and winter temperatures

Summer temperatures anomalies (Fig. 4) are characterised by a complex pattern throughout the entire Holocene but with a predominant NE–SW boundary separating warmer Scandinavia and Central Europe from cooler Eastern Europe and Italy. The Early Holocene (12–9 ka) was about 2 °C cooler than present, apart from the Alps and Lapland where temperatures warmer than the late pre-industrial were already present at 12 ka and remained a constant feature throughout much of the Holocene. Note that the chronological uncertainty means that the 12 ka map does not precisely capture conditions during the Younger Dryas cooling, and will also include elements of the early Holocene warming (see also Section 4.2). From 7 ka onwards, Central and Northern Europe became warmer, peaking at 7 ka and 2 ka when temperatures were up to 2 °C warmer in Scandinavia. The Mediterranean area was mainly cooler throughout the Holocene but with areas of Iberia showing alternating cooler and warmer periods.

Winter temperature anomalies (Fig. 5) were generally warmer in Northern Europe and cooler in Southern Europe, apart from the start of the Holocene where a general cooling was present all over Europe with temperatures more than 4 °C below late preindustrial in northwestern Europe, the British Isles, and the now submerged Doggerland region in the North Sea. From 10 ka to 9 ka, Central and Northern Europe were characterised by a gradual winter warming (up to 2 °C), which was most pronounced over Fennoscandia. At 8 ka, the warming intensified and extended laterally to Eastern Europe and France, peaking at 7 ka when the highest winter temperature anomalies of the Holocene are recorded in Northern Europe. During the mid-Holocene, winter temperatures were 1–2 °C higher in the Fennoscandian lowlands and up to 3 °C higher at elevation in the Norwegian mountains. From 4 ka onwards, temperature anomalies gradually decrease in Central Fennoscandia. In contrast, winter temperatures in Southern Europe were around 2 °C cooler than late preindustrial throughout much of the Holocene, excluding the last two millennia when anomalies relaxed towards present day values. A general feature present throughout the Holocene was the strong warming shown over the Armenian highland and Caucasian mountains. This warming may be the result of the interpolation process in areas with low data density and sudden changes in topography, and consequently is reflected in particularly high estimated uncertainties for this region (Fig. S5).

#### 3.2. Summer and winter precipitation

Overall during the Holocene, summers (Fig. 6) were wetter in Southern Europe and drier in Northern Europe as compared to the late preindustrial. In Southern Europe, the wettest period occurred between 8 ka and 6 ka where precipitation was ~20 mm/month higher than today over Italy and the North-Eastern Mediterranean, in contrast to Iberia which appears drier in many areas throughout most of the Holocene. Further north, a prominent feature that often

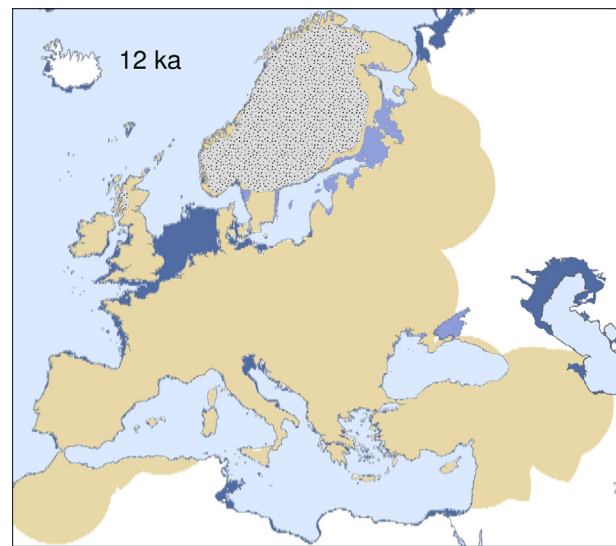


**Fig. 3.** European coastline at the onset of the Holocene relative to the present day, as a result of changes in sea level and isostatic readjustment. Dark blue areas are regions that at 12 ka were emerged from the sea, whilst light blue areas correspond to regions that at 12 ka were submerged by the sea. (For interpretation of the references to colour in this figure legend, the reader is referred to the web version of this article.)

occurs over the last 8000 years, and especially between 8 and 7 ka, but also at 2 ka, is a contrasting west–east moisture gradient over the Scandes mountains. This appears to show an orographic rain-shadow effect, with the windward western side of the mountains being wetter when the eastward leeward side is drier.

Winter precipitations anomalies (Fig. 7) show a general pattern through the Holocene characterised by a NW–SE boundary separating drier South-Western Europe from wetter Northern and Eastern Europe. Only at the start of the Holocene (12–10 ka) was Europe characterised by extensive dry conditions (~30 mm/month) that persisted until 9 ka, though with less magnitude and spatial extent. In the early Holocene only Poland was wetter already at 11 ka, expanding gradually to Fennoscandia at 9 ka, to Central Europe at 8 ka and to Southern Europe at 7 ka. The wettest period of the Holocene occurred at 7 ka with precipitation more than 20 mm/month higher than present over many Northern areas. Similarly to summer precipitation, a contrasting west–east gradient in winter precipitation can frequently be observed during the Holocene over the Scandes mountains.

#### 3.3. Other climate parameters

Also included in our climate reconstructions are mean annual temperature and total annual precipitation, growing degree-days above 5 °C (GDD5), and a measure of moisture balance calculated as the difference between annual precipitation minus evaporation (P–E). Of these only annual temperature and precipitation are corrected for isostatic adjustment because GDD5 and P–E were not available for the high resolution modern climate dataset that was used for isostatic correction. All of these additional climate variables are presented in the [supplementary information](#). GDD5 (Fig. S1) and mean annual temperature (Fig. S2) show a very similar pattern to summer temperature, with some small differences over the Eastern part of Europe and locally in Fennoscandia. Total annual precipitation (Fig. S3) anomalies are very similar to those shown for winter precipitation. P–E anomalies (Fig. S4) show a somewhat complex pattern with low water availability (~5 mm/day) during

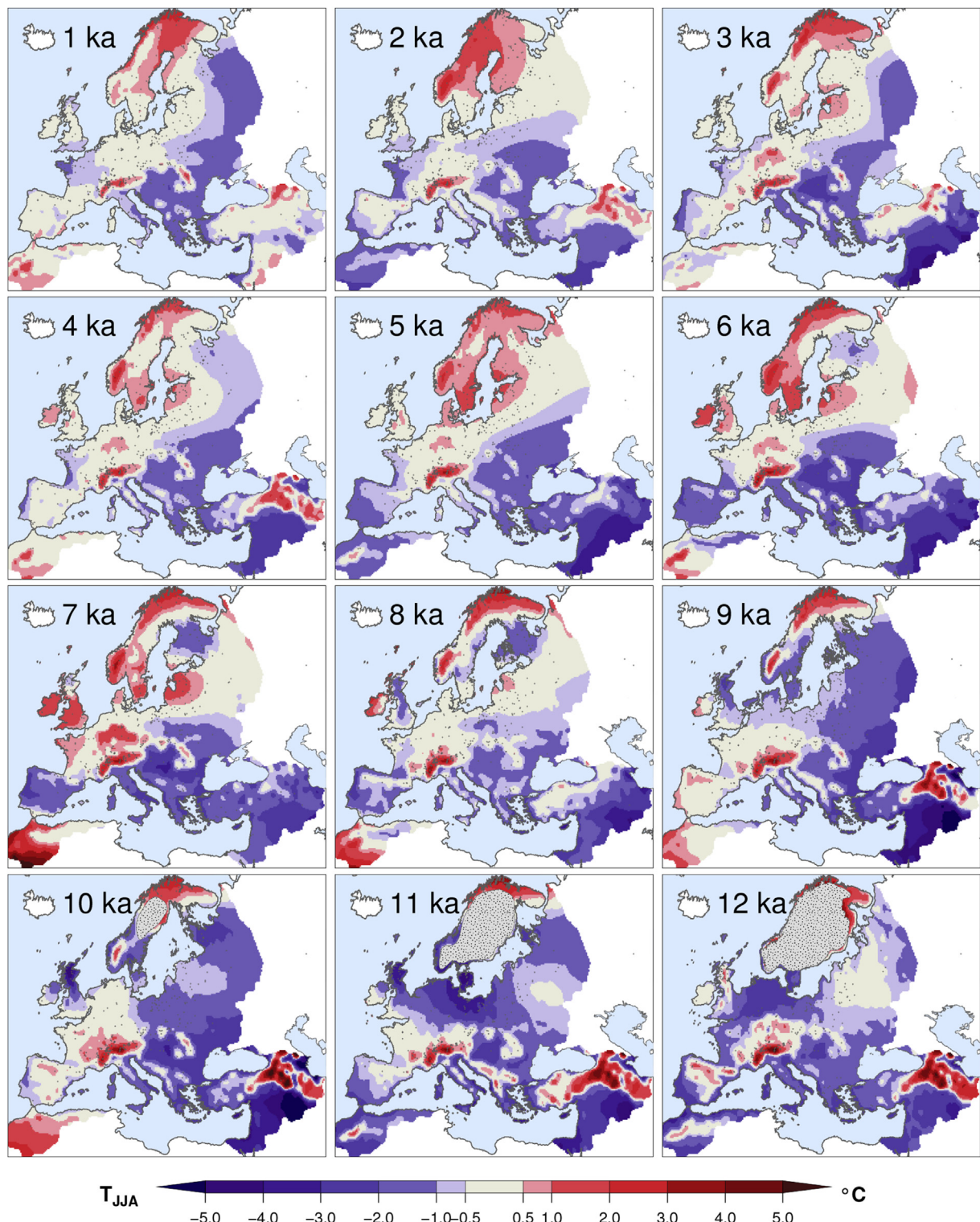


**Fig. 4.** Reconstructed Holocene summer (JJA) temperature anomalies ( $^{\circ}\text{C}$ ) relative to the pre-industrial (100 BP) period and corrected for isostatic rebound. Changes in coastline and topography as well as ice sheet extent are included. Interpolated climate values were limited to a distance of 500 km from the nearest pollen site location (grey crosses). Confidence limits are shown in [Supplementary Fig. S5](#).

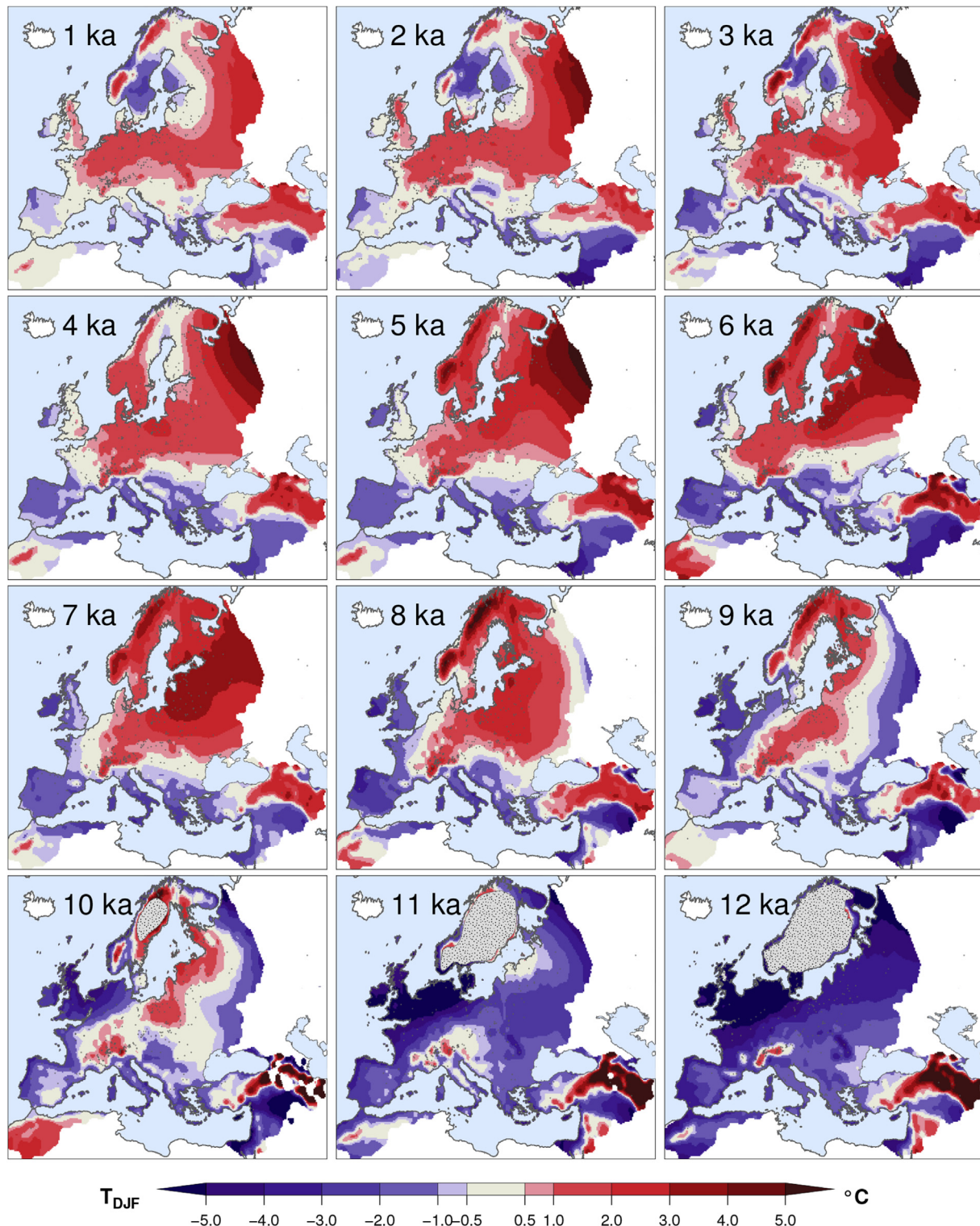


**Fig. 5.** As for Fig. 4, but showing reconstructed Holocene winter (DJF) temperature anomalies ( $^{\circ}\text{C}$ ). Confidence limits are shown in Supplementary Fig. S6.

the Early Holocene from 12 ka to 11 ka. From 10 ka to 7 ka, a west–east gradient is present with drier South-Western Europe and wetter North-Eastern Europe. At 6 ka, wetter conditions expand almost all over Europe, determining the wettest period of the Holocene. At 5 ka, an area of limited water availability appears in Scandinavia and persists all the way to 1 ka with some extensions into Finland and Iberia.

#### 4. Uncertainties and evaluation against independent climate reconstructions

##### 4.1. Discussion of uncertainties

Before discussing our results, it is important to consider the uncertainties and assumptions involved in pollen-climate

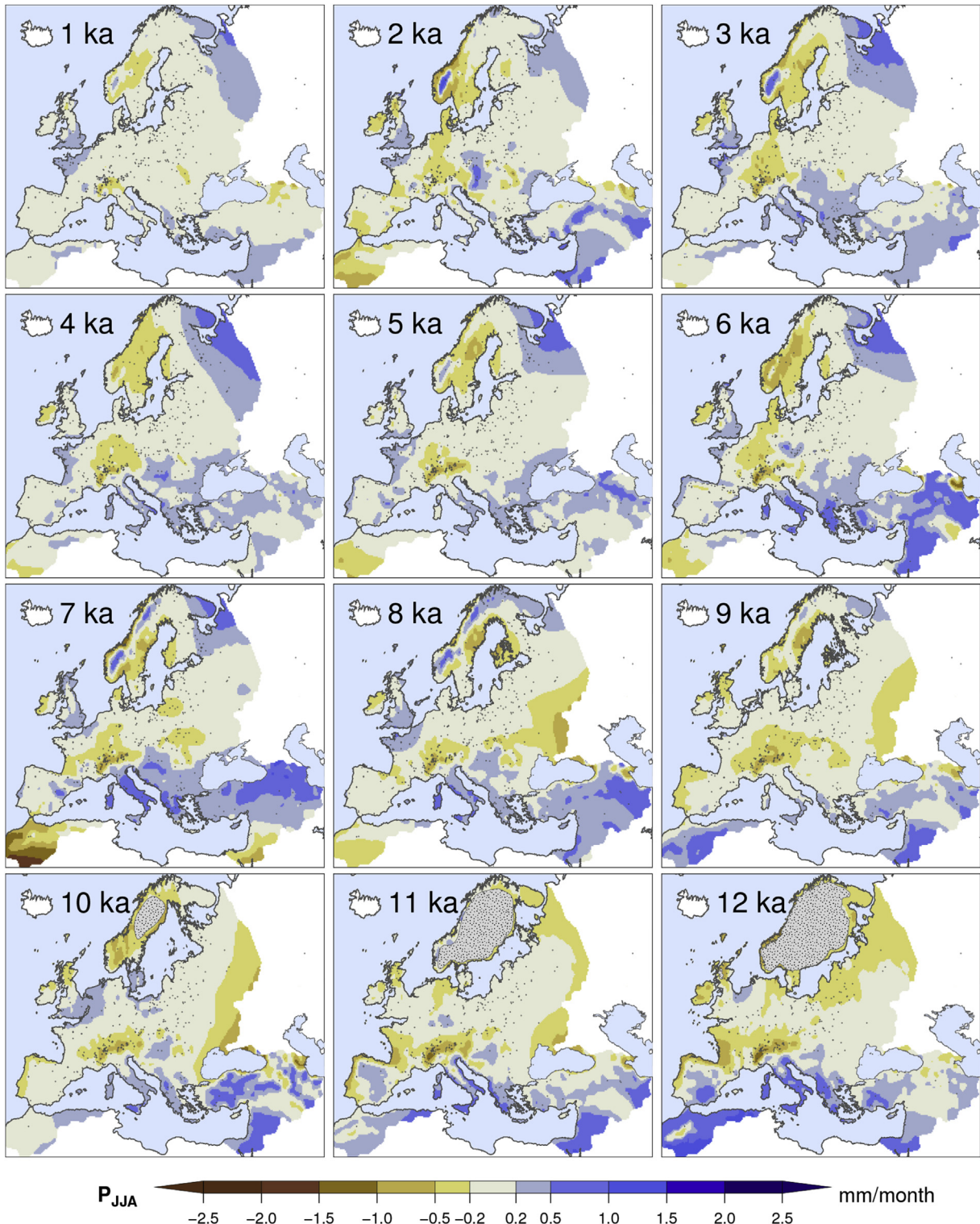


**Fig. 6.** As for Fig. 4, but showing reconstructed Holocene summer (JJA) precipitation anomalies (mm/month). Confidence limits are shown in Supplementary Fig. S7.

reconstructions. Many of these have been widely discussed in the literature (e.g., Seppä and Bennett, 2003; Birks and Seppä, 2004; Brewer et al., 2007a; Birks et al., 2010; Juggins and Birks, 2011; Juggins, 2013), but here we consider how they may be important in the context of our reconstruction and the methodology we have adopted:

#### 4.1.1. Anthropogenic disturbance

It has been suggested that the impact of anthropogenic activities during the last century might have led to an over-representation of non-arboreal pollen species in modern pollen training sets, which in turn might have caused misleading climate reconstructions (Birks et al., 2010). All pollen-climate reconstruction methods rely

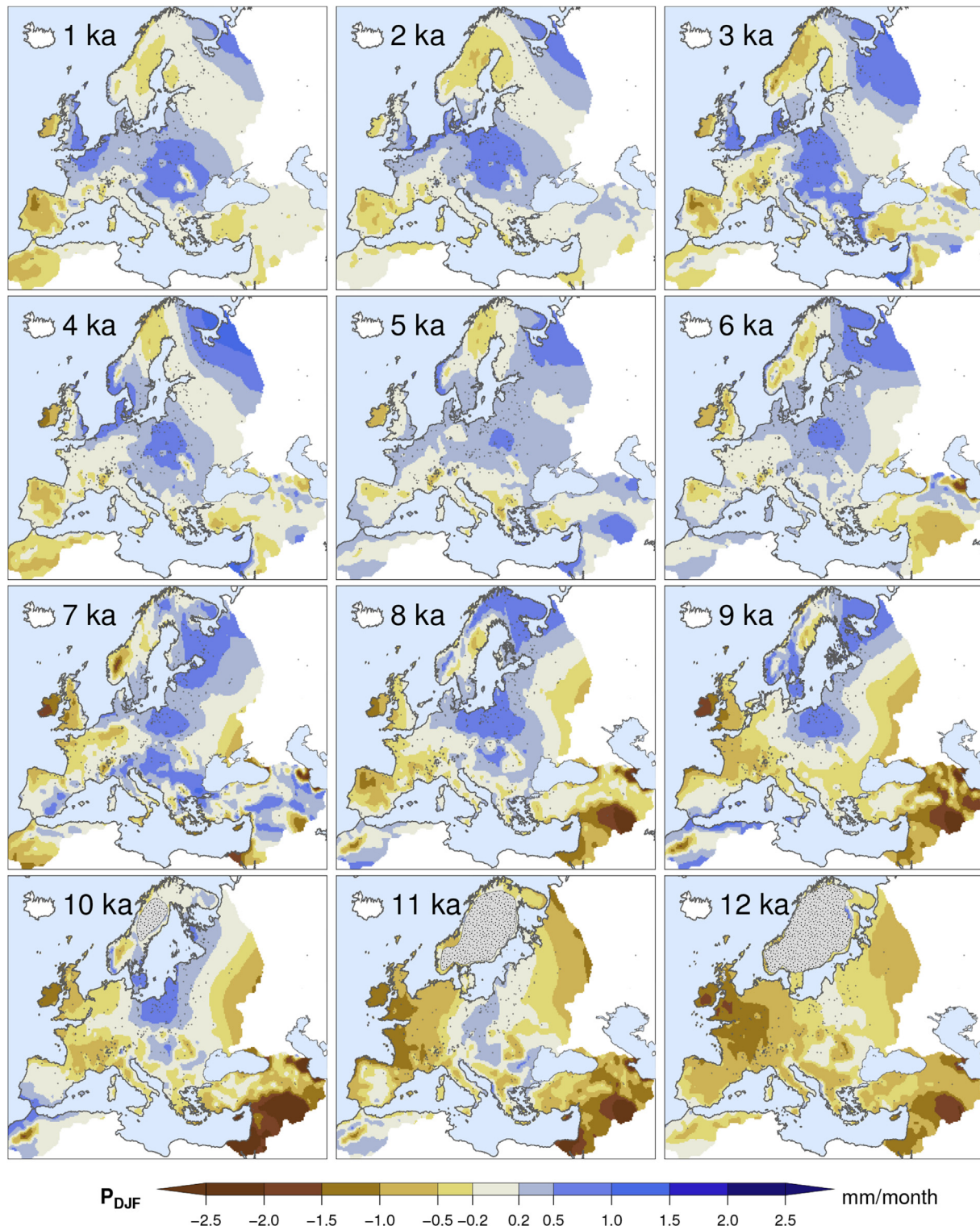


**Fig. 7.** As for Fig. 4, but showing reconstructed Holocene winter (DJF) precipitation anomalies (mm/month). Confidence limits are shown in Supplementary Fig. S8.

on an observed relationship between modern vegetation and climate, be this directly based on modern pollen surface samples or indirectly through maps of modern vegetation distributions. Without doubt the modern landscape of Europe is one that has been heavily influenced by both anthropogenic land cover and Holocene climate change. Nevertheless, at a continental scale, the modern vegetation distribution is still considered to be largely the

result of underlying climatic controls. This is also shown in analysis of continental scale modern pollen surface sample datasets, including our own analysis, which consistently demonstrate a statistically significant relationship between vegetation and climate in the modern human-impacted landscape (Huntley and Prentice, 1988; Huntley, 1990b, 1993; Cheddadi et al., 1997; Davis et al., 2003; Barboni et al., 2004; Gritti et al., 2004; Bordon et al.,

2009; Peyron et al., 2011). This is despite the fact that the European continent is among the most highly influenced by anthropogenic land cover change since at least the mid-Holocene (Kaplan et al., 2009, 2011).

In fact, the problem of the vegetation–climate relationship may more accurately be seen the opposite way around, in that it is a lack of human impact in the early and mid Holocene that may cause problems, because it is these more natural vegetation landscapes that are underrepresented in the modern training set. In any case, any dis-equilibrium between modern vegetation and climate will be largely captured in the estimated uncertainty of the reconstruction generated by the transfer function, which we have provided for all of our reconstructions. With this in mind, we have also applied to our reconstruction a quality control filter where we removed 3–5% of samples with the largest uncertainties. We also match fossil and modern samples based on an assemblage based on PFT classes and not individual taxa. This provides some measure of protection against anthropogenic disturbance since taxa changes caused by human disturbance within a PFT class, e.g., replacement of one temperate broadleaf forest tree species by another, will not influence the result (Davis et al., 2003).

#### 4.1.2. Lack of modern analogues

A common problem identified in MAT based pollen-climate reconstructions is finding a modern analogue within the training set for past vegetation encountered in the fossil record. This is a particular problem during periods in the past when vegetation was very different from today, such as during the LGM (Wu et al., 2007; Woillez et al., 2011), Lateglacial (Birks, 2003) and Last Interglacial (Kuhl and Litt, 2003; Kuhl et al., 2007), but it is considered less so for the Holocene. One way our method addresses this problem is again by using a PFT approach to analogue matching, as explained by Davis et al. (2003). This allows taxa that may not be present in the training set to find an analogue in other taxa present within the same PFT group. For instance, using the PFT approach we are able to find a modern analogue for *Buxus*, which was once an important forest forming plant in the Western Mediterranean (Di Domenico et al., 2013) but is rarely found today and was not present in our training set. This is because the PFT approach finds modern analogues for *Buxus* in other temperate broadleaf evergreen tree species such as *Hedera* and *Ilex*, which have similar plant functional traits. As already mentioned previously, the transfer function also generates a larger level of uncertainty when a poor analogue is encountered, as measured by the squared-chord distance (Overpeck et al., 1985). In filtering out those samples with the very highest uncertainties, we have also removed those samples with poor analogues in the training set. This filtering, however, only addresses the problem of poor analogues. A more difficult problem is that of making sure that the training set adequately samples the entire climate space in which a particular vegetation assemblage could exist. This is difficult to determine, since we are only able to observe the vegetation under modern climatic conditions. However in using a large surface sample dataset (81% larger than that used by Davis et al., 2003) that covers the major part of Europe, we hope to maximise the likelihood of finding both a modern vegetation and climatic analogue (Juggins and Birks, 2011).

#### 4.1.3. Spatial autocorrelation

The performance of a training-set is often estimated using cross-validation techniques, but performance can be overestimated as a result of spatial autocorrelation from geographically close analogues. Spatial autocorrelation problems occur mainly using MAT and Artificial Neural Network (ANN) techniques, because they are fitted to data locally rather than globally. MAT generally outperforms other reconstruction techniques when there is a strong

spatial autocorrelation in the modern training set, but it underperforms when modern datasets have a weak spatial autocorrelation (Birks et al., 2010). The extent of this problem has not generally been considered to be significant enough to limit the application of the MAT technique, and indeed the spatial structure in the data may still be an important function of the climatic response, especially at regional scales (Bartlein et al., 2010). In addition it is important to remember that the MAT technique also has many advantages over other alternative regression-based techniques such as WA and WA-PLS, particularly in continental scale analyses (Birks et al., 2010; Juggins and Birks, 2011). In evaluating our transfer function, we have tried to take account of the autocorrelation problem by adopting an n-fold-leave-one-out cross validation which provides a more reliable estimate of the model performance than simple leave-one-out cross-validation (Barrows and Juggins, 2005).

#### 4.1.4. Carbon dioxide

A major assumption in transfer-function based pollen-climate reconstructions is that the observed relationship between vegetation and climate today remained the same in the past. One factor that could significantly change this relationship however is the concentration of CO<sub>2</sub> in the atmosphere. For instance, during the LGM, CO<sub>2</sub> concentrations were around 50% lower (~185 ppm) than present (Monnin et al., 2001). Low atmospheric CO<sub>2</sub> concentrations are hypothesised to have led to compensatory changes in leaf physiology to meet the carbon demand of C<sub>3</sub> plants, including increases in stomatal density. Increases in stomatal conductance caused by low CO<sub>2</sub> directly and by increased stomatal density (Cowling and Sykes, 1999) would result in increased evapotranspirative water loss in plants. Under low CO<sub>2</sub> plants with conservative water use strategies, e.g., xerophytic taxa, may therefore have had a competitive advantage over, e.g., temperate and boreal forest trees (Harrison and Prentice, 2003). These changes in competitive balance have implications for paleoclimate reconstructions based on pollen data because modern analogues may not correctly capture the vegetation–climate relationship that existed in the past. Wu et al. (2007) found that reconstructed coldest month temperature anomalies during the LGM based on pollen data were significantly cooler if the CO<sub>2</sub> effect was not taken into account. Changes in CO<sub>2</sub> however during the Holocene were much smaller (~20 ppm, Indermuhle et al. (1999)) and Wu et al. (2007) concluded that they would not have had a significant impact on the vegetation and therefore their climate response.

#### 4.1.5. Migrational lag

Following a rapid and significant change in climate, plants may require some time to re-establish quasi-equilibrium with climate as they migrate and fill newly available niches in new locations. Since different plants may respond at different rates, this can result in new and unusual vegetation assemblages for which it may be difficult to find modern analogues (Huntley, 1990a). It may also result in a disconnection between vegetation and climate, with the reconstructed climate based on the slowly responding vegetation, and not on the rapidly changing climate. Migrational lag has traditionally been identified as a likely problem during the rapid climate shifts of the Lateglacial when it took centuries to millennia for vegetation to establish following deglaciation and climate warming over Northern Europe because of the distance from their glacial refugia in central and southern Europe the south. This problem is thought to be less of an issue however during the Holocene, when vegetation was already widely distributed and the speed and scale of climate change was somewhat less. That is not to say that migration lag is not important when looking at local scale studies with high temporal resolution, but it is generally considered

considerably less so when looking at millennial timescales considered in our study (Grimm and Jacobson, 2004; Bartlein et al., 2010). The PFT approach we use in our MAT technique has the further advantage of grouping both fast and slow dispersing/establishing taxa into a single functional group; this results in climate reconstructions that are less sensitive to the presence or absence of any particular taxon that could be affected by migrational lag.

#### 4.1.6. Reconstructed climate parameters

In this study we performed paleoclimate reconstructions for eight climate parameters. Birks et al. (2010) argues that it is often not possible to reconstruct multiple climate parameters from the same training set, although other authors consider that it is possible, at least for many of the parameters that we present here (Bartlein et al., 2010). Much depends on the particular parameter and size and spatial extent of the training set involved. Juggins and Birks (2011) suggest that pollen-climate reconstructions that make use of large unselected training sets spanning different vegetation and climatic regions should be less subject to the biases associated with much smaller datasets specifically selected along a strong environmental gradient. The independence of closely related parameters, such as mean winter temperature compared to the temperature of the coldest month for instance, would be difficult to demonstrate, and more often approximate to the same quantity (Bartlein et al., 2010). Here we do not attempt to justify our choice of parameters, other than to point to the extensive peer reviewed literature in which these parameters have already been applied.

#### 4.1.7. Covariance

Related to the problem of distinguishing the significance of any particular climatic parameter is the problem of covariance (Juggins, 2013). This occurs when the particular parameter being reconstructed is actually being driven by changes in a separate unrecorded parameter. For instance, the mid-Holocene summer cooling over Southern Europe reconstructed in pollen based studies (Huntley and Prentice, 1988; Davis et al., 2003; Wu et al., 2007) has been criticised by Renssen et al. (2012), who suggest that temperature reconstructions based on pollen data may be unreliable in the Mediterranean region where precipitation and not temperature may be the more dominant control. This is not a problem that has been demonstrated in the evaluation of transfer functions using modern pollen samples in the region, which give robust results for temperature reconstructions (Luterbacher et al., 2012), but as we have mentioned that is not to say such datasets cannot contain biases. Juggins (2013) discusses covariance and highlights the problem of distinguishing closely related climatic and other environmental variables using modern training sets. He identifies the problem as greatest in small training sets sampled along strong environmental gradients, but that problems are less with large continental-scale pollen training sets such as those used here, which are not pre-selected and which sample across multiple environmental gradients.

In this case it is possible to point to the results of inverse modelling studies in which a vegetation model is used to calculate the most likely climate for a given vegetation assemblage observed in the pollen record. For instance, Wu et al. (2007) reproduce the same summer cooling during the mid-Holocene that is found in studies using MAT, even though they use an inverse modelling method that does not rely on modern analogues. Alternatively, it is also possible to drive a vegetation model with the results of a climate model simulation, the results of which can also be compared directly with the vegetation shown in the pollen record. Again, the results show that models predict warmer dryer sclerophyllous vegetation over the Mediterranean consistent with the

simulated warmer than present summer temperatures, while the data actually indicates cooler temperate vegetation (Prentice et al., 1998; Wohlfahrt et al., 2004; Garzon et al., 2007).

#### 4.1.8. Non-climatic factors

Individual pollen records reflect a local vegetation assemblage that is subject to many influences apart from climate, including anthropogenic disturbance and migration lag that we have already mentioned, but also for instance disease, hydroseral succession, fire and edaphic factors. To this can be added the process of delivery of the pollen to the site and its incorporation and preservation in the sediment, as well as the coring, sampling, dating, laboratory analysis and counting involved in sampling and analysis. These processes carry many unaccounted uncertainties, and may add greatly to the noise in a record that makes discerning any underlying climate signal from any individual site difficult. The strength of our approach has been to integrate the records from many hundreds of sites and many thousands of samples into a single dataset spanning the entire European area for the entire Holocene. From this we have been able to raise the signal to noise ratio, and extract the underlying regional climatic signal from a series of individual records potentially influenced by many different local factors.

#### 4.2. Comparison with previous large-scale climate reconstructions

A number of European scale reconstructions have been made for the mid-Holocene period over the last 25 years, starting with the pioneering work of Huntley and Prentice (1988). These studies vary quite considerably in the size and nature of both fossil and modern pollen data, and the quality of the chronological control used. In comparing our current reconstruction with these previous studies, it is important to be aware of these differences, which are detailed more comprehensively in Mauri et al. (2014). For instance, reconstructions by Huntley and Prentice (1988), Guiot et al. (1993), Cheddadi et al. (1997) and Wu et al. (2007) use mostly data from Huntley and Birks (1983) for both fossil and modern pollen samples. The Huntley and Birks (1983) dataset only included a restricted number of 44 taxa and was largely composed of secondary digitised data from pollen diagrams published in the 1960's and 1970's. Dating control in many of these early pollen studies was often very limited, with around 33% of the sites in the Huntley and Birks (1983) dataset having no independent radiometric dating at all, being largely based on biostratigraphic correlation (Guiot et al., 1993). Uppermost core samples were also taken from this dataset in the compilation of training sets of modern pollen samples, although again the chronological control at many sites is weak, and the modern nature of the samples is not clear. In contrast, the Davis et al. (2003) reconstruction, which is mapped for the mid-Holocene in Brewer et al. (2007b), was based only on original primary count data consisting of the full taxa assemblage and used only sites with radiometric or other independently established chronologies.

Despite these differences, our reconstruction of mid-Holocene summer temperatures is very similar to that presented by Huntley and Prentice (1988) and Wu et al. (2007), with warmer temperatures over much of southern Scandinavia and central parts of Europe, and with cooler conditions over Southern Europe. We do not however find the same level of warming over the Balkans as these studies, which may be related to their use of data from Huntley and Birks (1983), which relied on sites with particularly poor chronological control in this area. Our reconstruction also does not show the strength of summer warming found in the Wu et al. (2007) reconstruction, although Wu et al. (2007) note that in evaluating their method they found a strong warm bias in summer temperatures. A pronounced feature of both our reconstruction and that of previous reconstructions is the strong

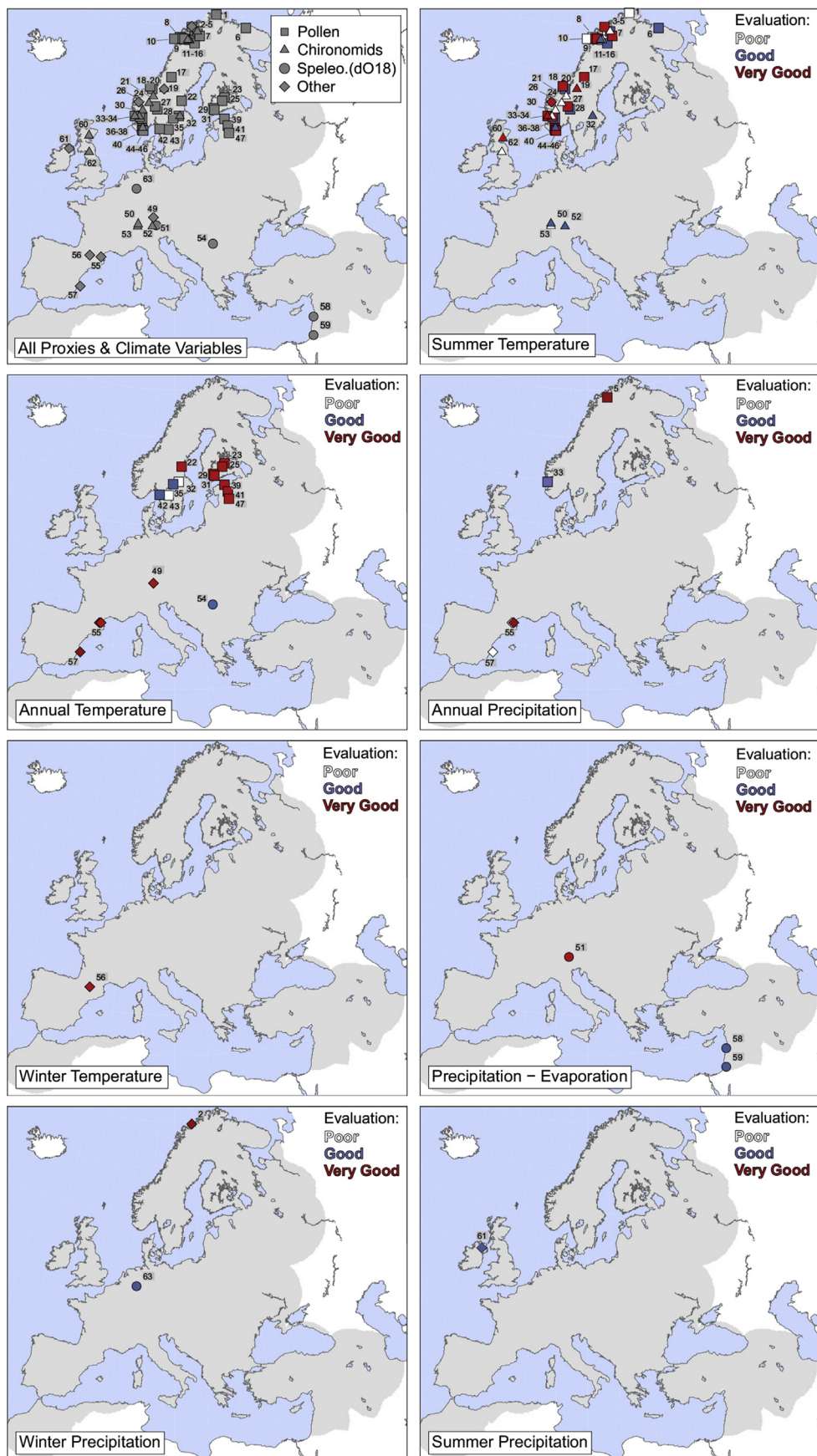


**Fig. 8.** Distribution of sites from previously published Holocene climate reconstructions used for the evaluation of the gridded climate reconstruction. Symbol colour indicates the level of agreement; very good (red), good (blue), white (poor). (For interpretation of the references to colour in this figure legend, the reader is referred to the web version of this article.)

warming in summer over the Alps. This was also identified by Huntley and Prentice (1988) who suggested that this may have been caused by a weaker environmental lapse rate as a result of an increase in atmospheric moisture. This is illustrated more clearly in Davis and Brewer (2008), who show how warming was greater at progressively higher altitudes. These warmer conditions in the Alps in the early–mid Holocene are however entirely consistent with evidence from other paleoclimate archives, which include reduced glacier extent (Grosjean et al., 2007; Goehring et al., 2011; Luetscher et al., 2011) and higher treeline altitudes (Nicolussi et al., 2005).

In winter in the mid-Holocene, we find that our reconstruction is also similar to previous reconstructions with a warming over northern Europe and cooling over southern Europe. However, whilst we reconstruct warming across most of central and eastern parts of northern Europe similar to Wu et al. (2007), Cheddadi et al. (1997) found maximum warming more to the east and Brewer et al. (2007b) more to the west of this area.

Mid-Holocene reconstructions of mean annual temperature by Wu et al. (2007) show a similar pattern to our own, indicating greatest warming over northern and central Europe and greatest cooling over southern. However, we reconstruct a greater level of warming over northern Scandinavia than Wu et al. (2007), which is more in agreement with Seppa et al. (2009).

Our reconstruction of growing degree days above 5 °C (GDD5) follows largely the same pattern of anomalies as for mean annual temperatures. This is comparable with Wu et al. (2007) including reduced GDD5 over southern Europe, but with slightly higher GDD5 over north-east Europe than found by Cheddadi et al. (1997) and Brewer et al. (2007b). Wu et al. (2007) also reconstructed seasonal and annual precipitation, but it is difficult to make comparisons with our own reconstruction because the scaling and presentation as dot maps makes it difficult to read the anomalies over Europe. Our reconstruction of P–E is also similar to Cheddadi et al. (1997) showing an excess of precipitation over eastern and southern Europe, but a deficit over northwest Europe including the UK. However, unlike Cheddadi et al. (1997) this deficit does not extend to the Scandes mountains in our reconstruction.

#### 4.3. Evaluation against independent climate reconstructions

We evaluated our reconstruction against 72 previously published quantitative Holocene climate reconstructions from 62 sites from across Europe (Fig. 8). We did this by comparing each site record against the nearest grid point of our one-degree gridded dataset, a maximum distance of 60–70 km. The range of paleoclimate proxies we used in our comparison includes chironomids,  $\delta^{18}\text{O}$  from speleothems and lake ostracods, bog-oaks, glacio-lacustrine sediments and wood anatomy. We also include other pollen-based studies where these have been based on alternative reconstruction methods (e.g., WA-PLS) or significantly different training sets. We selected only those studies and archives that provided quantitative climate reconstructions directly comparable with one of the climatic parameters in our own reconstruction. We do not include reconstructions based on essentially qualitative or semi-quantitative methods, such as lake level reconstructions, nor do we include studies that cover only a small part of the Holocene period. Isotope  $\delta^{18}\text{O}$  studies are included where the authors make an explicit climatic interpretation. We also only include studies where we could obtain the original data either from public archives such as the NOAA palaeoclimate website (<http://www.ncdc.noaa.gov/data-access/paleoclimatology-data/datasets>), or from the authors themselves (Brooks et al., 2007; Constantin et al., 2007; Dalton et al., 2005; Hammarlund et al., 2004; Heiri et al., 2003; Ilyashuk et al., 2011; Langdon et al., 2004; Larocque-Tobler et al.,

2010; Nesje and Kvamme, 1991; Orland et al., 2012; Pla and Catalan, 2005; Terral and Arnold-Simard, 1996; Verheyden et al., 2008; von Grafenstein et al., 1999). We have tried to include as many studies as possible to provide a representative analysis, but recognise that this list may not be exhaustive. A full list of sites and studies is provided in Table S1, with the comparison plots shown in Supplementary Fig. S10.

Most of the independent climate reconstructions from Scandinavia did not compensate for isostatic adjustment, and we only include this where this was included as part of the original analysis [sites 19, 21, 24, 26, 30, 34]. Anomalies for all sites were recalculated relative to the preindustrial period to ensure compatibility with our own reconstruction. We assess the comparability of the grid point and independent reconstruction for each site and climate variable by plotting the two time-series together on the same figure (see example shown in Fig. 9). Due to the variable nature of the sampling interval, estimation of uncertainty, and in some cases the units used, we estimated the fit based on qualitative criteria on a three-point scale ranging from poor to good and very good. Where the two reconstructions intersected for the majority of the record, then we classified this as ‘very good’, where they were within one standard deviation of the mean variance of the independent reconstruction for the majority of the record, we classified this as ‘good’ and where the two records were either clearly outside this limit or of opposite sign, then we classified this as a ‘poor’ fit. However, it should be noted that any differences between our reconstruction and the independent archives are almost always within the combined uncertainty of the methods, even where the correspondence is categorised as ‘poor’.

The largest number of independent reconstructions was for summer temperature (Fig. S10.2), with a total of 45 records, mainly from Northern Europe (27 from pollen, 17 from chironomids and 1 from glacio-lacustrine sediments and palaeobotanical data). In most cases, these are reconstructions of mean July temperature, which we interpret as commensurate with our reconstruction of mean summer (JJA) temperature, which is also the conclusion of Bartlein et al. (2010). Overall, the independent climate reconstructions compared well with our reconstruction. Of the pollen-based reconstructions we found 21 of the 27 comparisons were either good or very good, while only 6 showed a poor match. This is perhaps not surprising since our reconstruction used many of the same sites and surface samples, although sites such as Grostjørna [44], Reiersdalvatnet [45], Dalane [46] and Svanåvatnet [17] show a ‘very good’ match even though they are not included in our fossil dataset. One of the sites that we classified as ‘poor’ was that of Dalmutladdo [5] in Northern Norway, which has been reconstructed by both Seppa et al. (2009) [5a] and Bjune et al. (Bjune et al., 2005) [5b]. However, while the comparison with Seppa et al. (2009) climate reconstruction (Dalmutladdo 5a) shows a systematic offset through the Holocene resulting in a ‘poor’ fit, the Bjune et al. (2005) reconstruction (Dalmutladdo 5b) shows a good match over at least the last 7000 years. Both studies use the same fossil pollen data, and both use the same WA-PLS transfer function method, but there are substantial differences in the modern surface sample dataset. The Bjune et al. (2005) study used a data set of 304 pollen surface samples taken from Norway, northern Sweden and Finland, while the Seppa et al. (2009) study used a dataset of 283 samples taken from Norway and northern Sweden only. The explanation for the difference between these two reconstructions therefore appears to be the result of the Finland samples, which may have provided warmer summer analogues in the case of the Bjune et al. (2005) study. This is in contrast to the Seppa et al. (2009) study where analogues would have been restricted to the more maritime region of western Scandinavia, which experiences cooler summers. The same problem may account for the

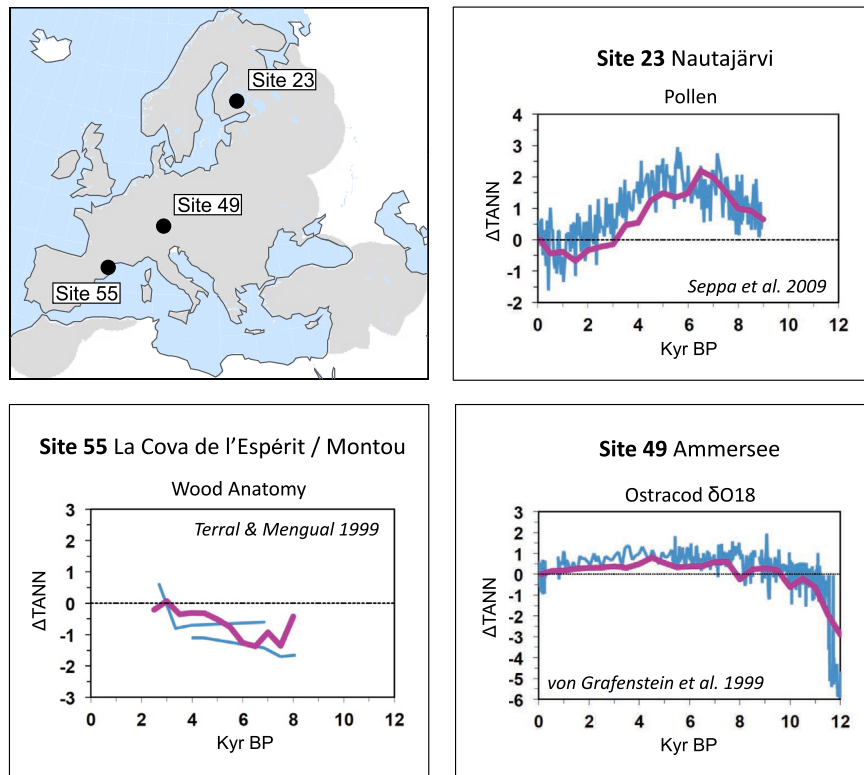


**Fig. 9.** An example showing evaluation of the gridded climate reconstruction for mean annual temperature (TANN) at three different sites and for three different paleoclimate archives. The thin line represents the published reconstruction, and the thick bold line is the grid-based reconstruction presented here. Site 55 shows two published reconstructions from adjacent locations. All three examples show a very good match with the grid-based reconstruction, which reproduces the contrasting temperature history shown at each site. This indicates strong mid-Holocene warming at the northern Europe site, moderate warming at the central Europe site, and mid-Holocene cooling at the southern Europe site.

consistently cooler summer temperatures reconstructed by [Seppa et al. \(2009\)](#) at other sites that we have compared with our own reconstruction [1,4a,6,8,9,10,16,36,37,38], and illustrates the importance of ensuring a training set of modern samples that is representative of both vegetation and climate space (see Section 4.1.2).

Comparisons of summer temperatures with chironomid based reconstructions showed a very good match for 6 sites, a good match for 2 sites and a poor match for 9 sites. Large discrepancies between pollen-based reconstructions and those based on chironomid reconstructions are not just confined to our own study, but can also be seen at Toskaljavri [4] and Vestre Øykjamyrtyrøn [34b] where pollen reconstructions have also been made by other authors. This pollen-chironomid problem has been previously identified in Scandinavia ([Bakke et al., 2005; Velle et al., 2005, 2010](#)). In deciding which may be the more reliable proxy, it has been noted that pollen reconstructions show a high degree of spatial consistency in Scandinavia as might be expected from climate change observed in the instrumental record, while chironomid-based reconstructions show much greater variability. This can be shown most clearly where analysis has been performed at adjacent sites, and where chironomid based reconstructions show large differences ([Velle et al., 2010](#)), for instance at sites [13, 14a, 15] and [33b, 34]. It has also been noted that chironomid records tend to consistently reconstruct cooler summer temperatures than pollen ([Birks et al., 2010](#)), such as at lake Lake Gilltjärnen [32] in north-central Sweden as shown by [Antonsson et al. \(2006\)](#). This also appears to be the case at Hinterburgersee [53] in the Swiss Alps, where our reconstructed summer temperatures also appear around 2–3 °C warmer.

Our reconstruction of mean annual temperature anomalies (Fig. S10.1) was compared against 17 independent reconstructions

from both north and south Europe, and based on a wide variety of proxies including pollen, macrofossils, and d18O from speleothems and ostracods. Overall, 12 records were classified as very good, 5 good, and 0 poor. As with summer temperatures, the majority of the reconstructions use pollen data (12 records), and although the fit is better than for summer temperature, many of the records also show a systematic offset. The difference in this case is that the reconstructions of annual temperatures often appear warmer [sites 22, 31, 35, 39, 41, 43, 47], whereas they appeared cooler in summer. All the pollen records come from the study by [Seppa et al. \(2009\)](#), and again as discussed previously, the reason may be related to the modern surface samples in the training set. For summer temperatures [Seppa et al. \(2009\)](#) used a dataset that mainly came from western Fennoscandia that has cooler summers than eastern Fennoscandia, but for annual temperatures they used a dataset from eastern Fennoscandia (Finland, Estonia, Sweden), which has higher mean annual temperatures than western Fennoscandia. The use of different sets of samples from different climatic regions could therefore explain the difference with our own reconstruction, which is based on samples from both regions. Both our own reconstruction, and those of [Seppa et al. \(2009\)](#) reconstruct a thermal maximum of around 2 °C warmer than late preindustrial in the early to mid Holocene at sites in Northern Europe, but reconstructions from further south show a different pattern, which we also find in our own reconstruction. At Lake Ammersee [49] in southern Germany an ostracod based δ18O record shows a much more restricted early–mid Holocene warming of less than 1 °C, whilst a δ18O speleothem record from Poleva Cave [54] in Romania was interpreted by the authors as showing no early–mid Holocene warming at all, but instead a warming trend from early to late Holocene. We also reproduce a similar cooler mid-Holocene found

at Montou and Cova de l'Espirit [55] in north-east Spain, and at Cova de les Cendres [57] in south-eastern Spain, both of which were based on changes in olive wood structure using carbonised macrofossil remains. These differences in Holocene temperature trends between north, central and south Europe in both our own and these other studies are illustrated in Fig. 9.

For the other climate variables we considered, fewer independent reconstructions exist. We found only one Holocene reconstruction of winter temperatures (Fig. S10.3), located at Lake Redon [56] in Northern Spain that was based on chrysophyte cysts. This we classified as a 'very good' fit to our own reconstruction, where we also showed a warming trend throughout the Holocene. These cooler conditions in the early–mid Holocene at this southern Europe site contrasts with those that we reconstruct over northern Europe, where we found the winter warming in the mid-Holocene was even greater than that found in summer. Independent support for this strong winter warming over northern Europe comes from the presence of Mediterranean Ostracod species in mid-Holocene marine sediments in northern Denmark, which suggest coldest month sea surface temperatures 5–6 °C warmer than present in the mid-Holocene (Vork and Thomsen, 1996). Similar warming is also suggested by the presence of fish remains from species normally associated with warmer waters found at the same place and dating from the mid-Holocene (Enghoff et al., 2007). Of other independent pollen-based reconstructions, Brown et al. (2012) recently published a reconstruction for sites in Denmark that also indicate a stronger warming in winter than in summer, and with mid-Holocene temperature anomalies of around +2 °C for the region that are comparable with our reconstruction.

We compared our reconstructions of total annual precipitation (Fig. S10.4) with two pollen-based reconstructions at Dalmutladdo (5b) in Northern Norway and Vestre Øykjamyrkjøn (33) in Southern Norway, which both showed a 'very good' match although Dalmutladdo shows substantial high-frequency variability that is not captured in our reconstruction. We also compared our results against two records from Spain, from Montou and Cova de l'Espirit [55] in the northeast, and Cova de les Cendres [57] in the southeast; these are based on the same carbonised macrofossil material used to reconstruct annual temperature described previously. All of these sites show higher mean annual precipitation in the mid-Holocene in agreement with our reconstruction, although the absolute levels at two of the sites are higher.

In terms of summer precipitation (Fig. S10.5), we found a good match against a palaeoclimate record based on oaks buried in Irish bogs [61], with more bog oaks in the mid Holocene suggesting relatively drier summers. The original authors interpret the record as a measure of summer season moisture balance (P–E) (Turney et al., 2005; Charman, 2010), but since our dataset does not include a direct measure of seasonal P–E, we believe summer precipitation should be comparable given that summer temperature would not be a strong control on moisture balance in the temperate climate of Ireland.

Evaluation of our winter precipitation reconstruction could be seen as particularly important given that this climate parameter showed the weakest predictive skill (Table 1). In fact our reconstruction shows a very good match with independent reconstructions based on a speleothem  $\delta^{18}\text{O}$  record from Bunker Cave [63] in Northern Germany (Fohlmeister et al., 2012), and for the site of Aspvatnet [2] in Northern Norway that was based on analysis of glacio-lacustrine sediments and regional pollen and chironomid temperature reconstructions. The published Aspvatnet precipitation reconstruction is for October–April snowfall (Bakke et al., 2005), which we converted to water equivalent by dividing by a factor of 10, and then to mm/month by dividing by 7. The very good quantitative agreement with our own reconstruction provides

support for the ability of transfer function to reconstruct winter precipitation in a region where much of this falls as snow, and where vegetation is mainly dormant in winter.

Finally, we compared our Precipitation–Evaporation (P–E) reconstruction against  $\delta^{18}\text{O}$  speleothem records from Jeita Cave [58] in Lebanon and Soreq Cave [59] in Israel, and from Spannagel Cave [51] in Austria. We classified the fit in all cases as 'good', although it must be recognised that the authors of these studies do not directly interpret these records as P–E, but as a function of both temperature and precipitation. There does not appear to be any consistent climatic interpretation of the  $\delta^{18}\text{O}$  signal in speleothems (Lachnit, 2009), with sites relatively close to one another in central Europe for instance being variously interpreted in terms of winter precipitation at Bunker Cave [63] in Germany, annual temperature at Poleva Cave [54] in Romania, or temperature and precipitation at Spannagel Cave [51] in Austria. Often interpretation is based on modern monitoring of cave waters, but to extend this into the past means making assumptions about the stationarity of seasonality, snow cover, vegetation cover, and precipitation source and trajectory, and other variables which are difficult to know with confidence, particularly over as long a period as the Holocene.

In summary, we find that our reconstruction largely reproduces the record of Holocene climate change found in other studies. Holocene climate change was not uniform across Europe and different regions experienced not only different magnitudes of change, but also change of an entirely different sign. We find that we are able to reproduce these different regional responses revealed in other studies, finding for instance a mid-Holocene warming over northern Europe and cooling over southern Europe (such as shown in Fig. 9). Overall we find a 'good' or 'very good' match in 78% of studies, and a poor match in 22%. Of the site records classified as a poor match, more than half were based on chironomids, whilst more than half of those classified as good or very good were based on pollen. Differences between reconstructions do not necessarily indicate that they are in error, but that they could also be sensitive to different aspects of the same climatic changes. For instance, chironomids have a life-cycle measured in weeks or months and are particularly sensitive to short-term minimum or maximum temperatures, whereas forest trees featured in pollen records may live for decades or even centuries and only show sensitivity to long-term change in mean climate over similar timescales. However, we would also expect that reconstructions from the same proxy from sites within the same climatic region should show a similar record of climatic change. In the case of pollen data, this inter-site reproducibility can be demonstrated (Seppa et al., 2009), but for other records this is more difficult given the limited number of studies available for most alternative proxies. One of the criticisms of chironomid reconstructions in Scandinavia has come from comparing records from nearby sites only to find that they show very different trends, perhaps indicating sensitivity to non-climatic factors such as trophic status (Velle et al., 2010). Brooks et al. (2012) have responded by suggesting that a study in Iceland has shown near-identical reconstructions from adjacent sites (Caseldine et al., 2006), whilst the differences noted in Scandinavia are nevertheless still within the uncertainties ( $\pm 1^\circ\text{C}$ ) of the reconstructions. Juggins and Birks (2011) has noted the difficulties in using small calibration datasets taken along a strong environmental gradient, as often used in many chironomid studies, because the propensity for misleading co-variance between environmental parameters can be large. This is less of a problem for large continental-scale datasets used in pollen-climate reconstructions such as we have used here, but smaller datasets may still cause other problems if only because they limit

the number of both vegetation and climate analogues. We have highlighted here differences between pollen-based reconstructions based on smaller regionally constrained training sets (Bjune et al., 2005; Seppä et al., 2009), and this problem may also explain the differences we find between our own reconstruction and those of other pollen-based studies.

## 5. Conclusions

We present a new improved pollen-based gridded Holocene climate reconstruction for Europe. This is presented at 1000 years time intervals for the last 12,000 years, and includes reconstructions of seasonal and annual temperature and precipitation, growing degree-days above 5 °C (GDD5), and a measure of moisture balance (P-E). We have used the same transfer function and 4-dimensional gridding methodology as Davis et al. (2003), but with a substantial improvement in data quality and extent. The modern pollen dataset has been increased by more than 80%, and the fossil pollen dataset by more than 50%, representing almost 60,000 individual pollen samples.

Our analysis takes account of post-glacial isostatic adjustment that we estimate resulted in a potential warming bias of up to +1–2 °C for parts of Fennoscandia in the early Holocene. We have also included sea level changes and other aspects of palaeogeography, revealing many features of the early Holocene European landscape that have since disappeared, such as the early-expanded Baltic sea/lake and the ancient Doggerland that now lies beneath the North Sea.

The reconstruction we present has undergone a series of quality control checks and full-error accounting of transfer function and interpolation uncertainties, which have allowed us to establish confidence limits for the dataset. Furthermore, we have evaluated our reconstruction against independent climate reconstructions on a site-by-site basis, including sites and archives that are not included in our dataset. Overall we find that our climate reconstruction largely reproduces the results of these independent studies, finding that 78% can be qualitatively classified as a good or very good match, and 22% as poor. Of the studies classified as poor, over half were based on chironomids, which other authors have identified as showing inconsistencies when used to reconstruct climate. Nevertheless, in almost all cases including those where the match was classified as poor, the degree of agreement falls well within the combined confidence limits of the two records, and may indicate that reconstructions may be more reliable than statistical uncertainty estimates based on modern training sets suggest.

Our climate reconstruction is freely available for download (see Acknowledgements), where we hope it will be used to evaluate the growing number of transient Holocene model simulations as well as provide climate data for other applications such as vegetation and land-use modelling. One focus for climate model evaluations would be the persistent data-model discrepancy over southern Europe in the mid-Holocene where models indicate summer warming, but the data indicates summer cooling. Similarly, we find that in our reconstruction the most important driver of interglacial warming in Europe have been changes in winter and not summer temperatures, an apparent paradox that is not consistent with current climate models simulations and traditional interpretations of Milankovitch theory (Mauri et al., 2014).

## Acknowledgements

The authors would like to thank all those who provided climate reconstructions used for the comparison, especially Heikki Seppä, Anne Elisabeth Bjune, Gaute Velle, Steve Brooks, Jens Fohlmeister, Natalie St. Amour, Jordi Catalan, Catherine Dalton, Oliver Heiri,

Elena Ilyashuk, Peter Langdon, Isabelle Larocque, Jean-Frederic Terral, Chris Turney, Sophie Verheyden. We also thank Richard Gyllencreutz for providing Early Holocene ice sheet maps of Northern Europe and David Frank, Heikki Seppä and Heinz Wanner for comments on earlier drafts of the manuscript. This study would not have been possible without the resources provided by the European Pollen Database and the PANGAEA data archive. Funding was provided by grants from the Swiss National Science Foundation (PP0022\_119049), the Italian Ministry of Research and Education (FIRB RBID08LNFI), and the European Research Council (COEVOLVE 313797). Full results are available to download as netcdf and tiff files from [http://arve.unil.ch/pub/EPOCH-2\\_Mauri\\_et.al\\_QSR.tar.gz](http://arve.unil.ch/pub/EPOCH-2_Mauri_et.al_QSR.tar.gz). Requests for further information should be addressed to the corresponding author.

## Appendix A. Supplementary data

Supplementary data related to this article can be found at <http://dx.doi.org/10.1016/j.quascirev.2015.01.013>.

## References

- Amante, C., Eakins, B.W., 2009. ETOPO1 1 Arc-minute Global Relief Model: Procedures, Data Sources and Analysis. NOAA Technical Memorandum NESDIS NGDC-24.
- Antonsson, K., Brooks, S.J., Seppä, H., Telford, R.J., Birks, H.J.B., 2006. Quantitative palaeotemperature records inferred from fossil pollen and chironomid assemblages from Lake Gilltjärnen, northern central Sweden. *J. Quat. Sci.* 21, 831–841.
- Bakke, J., Dahl, S.O., Paasche, O., Lovlie, R., Nesje, A., 2005. Glaciation fluctuations, equilibrium-line altitudes and palaeoclimate in Lyngen, northern Norway, during the Lateglacial and Holocene. *Holocene* 15, 518–540.
- Barboni, D., Harrison, S.P., Bartlein, P.J., Jalut, G., New, M., Prentice, I.C., Sanchez-Goni, M.-F., Spessa, A., Davis, B.A.S., Stevenson, A.C., 2004. Relationships between plant traits and climate in the Mediterranean region: a pollen data analysis. *J. Veg. Sci.* 15, 635–646.
- Barrows, T.T., Juggins, S., 2005. Sea-surface temperatures around the Australian margin and Indian Ocean during the last glacial maximum. *Quat. Sci. Rev.* 24, 1017–1047.
- Bartlein, P.J., Harrison, S.P., Brewer, S., Connor, S., Davis B.A.S., Gajewski, K., Guiot, J., Harrison-Prentice, T.I., Henderson, A., Peyron, O., Prentice, I.C., Scholze, M., Seppä, H., Shuman, B., Sugita, S., Thompson, R.S., Vlaar, A.E., Williams, J., Wu, H., 2010. Pollen-based continental climate reconstructions at 6 and 21 ka: a global synthesis. *Clim. Dyn.* 37, 775–802.
- Birks, H.H., 2003. The importance of plant macrofossils in the reconstruction of Lateglacial vegetation and climate: examples from Scotland, western Norway, and Minnesota, USA. *Quat. Sci. Rev.* 22, 453–473.
- Birks, H.J.B., Heiri, O., Seppä, H., Bjune, A., 2010. Strengths and weaknesses of quantitative climate reconstructions based on late-Quaternary biological proxies. *Open Ecol. J.* 3, 68–110.
- Birks, H.J.B., Seppä, H., 2004. Pollen-based reconstructions of late-Quaternary climate in Europe – progress, problems, and pitfalls. *Acta Palaeobot.* 44, 317–334.
- Bjune, A.E., Bakke, J., Nesje, A., Birks, H.J.B., 2005. Holocene mean July temperature and winter precipitation in western Norway inferred from palynological and glaciological lake-sediment proxies. *Holocene* 15, 177–189.
- Bonfils, C., de Noblet-Ducoudre, N., Guiot, J., Bartlein, P., 2004. Some mechanisms of mid-Holocene climate change in Europe, inferred from comparing PMIP models to data. *Clim. Dyn.* 23, 79–98.
- Bonsall, C., Macklin, M.G., Anderson, D.E., Payton, R.W., 2001. Climate change and the adoption of agriculture in North-West Europe. *Eur. J. Archaeol.* 5, 7–21.
- Bordon, A., Peyron, O., Lézine, A.M., Brewer, S., Fouache, E., 2009. Pollen-inferred Late-Glacial and Holocene climate in southern Balkans (Lake Maliq). *Quat. Int.* 200, 19–30.
- Braconnot, P., Harrison, S., Kageyama, M., Bartlein, J., Masson, V., Abe-Ouchi, A., Otto-Bliesner, B., Zhao, Y., 2012. Evaluation of climate models using palaeoclimatic data. *Nat. Clim. Change* 2, 417–424.
- Brewer, S., Guiot, J., Barboni, D., 2007a. Pollen data as climate proxies. In: Elias, S.A. (Ed.), *Encyclopedia of Quaternary Science*. Elsevier, pp. 2498–2510.
- Brewer, S., Guiot, J., Torre, F., Davis, B.A.S., Stevenson, A.C., 2007b. Mid-Holocene climate change in Europe: a data-model comparison. *Clim. Past* 3, 499–512.
- Brooks, S.J., Axford, Y., Heiri, O., Langdon, P.G., Larocque-Tobler, I., 2012. Chironomids can be reliable proxies for Holocene temperatures. A comment on Velle et al. (2010). *Holocene* 22, 1495–1500.
- Brooks, S.J., Langdon, P.G., Heiri, O., 2007. The Identification and Use of Palaeartic Chironomidae Larvae in Palaeoecology. Quaternary Research Association, London. ISBN 0907 780 717.

- Brown, K.J., Seppa, H., Schoups, G., Fausto, R.S., Rasmussen, P., Birks, H.J.B., 2012. A spatio-temporal reconstruction of Holocene temperature change in southern Scandinavia. *Holocene* 22, 165–177.
- Bruckner, H., Kelterbaum, D., Marunchak, O., Porotov, A., Vott, A., 2010. The Holocene sea level story since 7500 BP – lessons from the Eastern Mediterranean, the Black and the Azov Seas. *Quat. Int.* 225, 160–179.
- Carlson, A.E., 2011. Ice sheets and sea level in Earth's past. *Nat. Educ. Knowl.* 3, 3.
- Caseldine, C., Langdon, P., Holmes, N., 2006. Early Holocene climate variability and the timing and extent of the Holocene thermal maximum (HTM) in northern Iceland. *Quat. Sci. Rev.* 25, 2314–2331.
- Castiglioni, P., 2005. Zero-padding. In: Armitage, P., Colton, T. (Eds.), *Encyclopedia of Biostatistics*. John Wiley & Sons, Ltd.
- Charman, D.J., 2010. Centennial climate variability in the British Isles during the mid-late Holocene. *Quat. Sci. Rev.* 29, 1539–1554.
- Cheddadi, R., Yu, G., Guiot, J., Harrison, S.P., Prentice, I.C., 1997. The climate of Europe 6000 years ago. *Clim. Dyn.* 13, 1–9.
- Collins, P.M., Davis, B.A.S., Kaplan, J.O., 2012. The mid-Holocene vegetation of the Mediterranean region and southern Europe, and comparison with the present day. *J. Biogeogr.* 39, 1848–1861.
- Combouret, Nebout, N.C., Peyron, O., Dormoy, I., Desprat, S., Beaudouin, C., Kotthoff, U., Marret, F., 2009. Rapid climatic variability in the west Mediterranean during the last 25 000 years from high resolution pollen data. *Clim. Past* 5, 503–521.
- Constantin, S., Bojar, A.V., Lauritzen, S.E., Lundberg, J., 2007. Holocene and Late Pleistocene climate in the sub-Mediterranean continental environment: a speleothem record from Poleva Cave (Southern Carpathians, Romania). *Palaeogeogr. Palaeoclimatol. Palaeoecol.* 243, 322–338.
- Cowling, S.A., Sykes, M.T., 1999. Physiological significance of low atmospheric CO<sub>2</sub> for plant-climate interactions. *Quat. Res.* 52, 237–242.
- Dalton, C., Birks, H.J.B., Brooks, S.J., Cameron, N.G., Evershed, R.P., Peglar, S.M., Scott, J.A., Thompson, R., 2005. A multi-proxy study of lake-development in response to catchment changes during the Holocene at Lochnagar, north-east Scotland. *Palaeogeogr. Palaeoclimatol. Palaeoecol.* 221, 175–201.
- Davis, B.A.S., Brewer, S., 2008. Orbital forcing and the role of the latitudinal insolation/temperature gradient. *Terra Nostra* 2, 57–58.
- Davis, B.A.S., Brewer, S., 2009. Orbital forcing and the role of the latitudinal temperature/insolation gradient. *Clim. Dyn.* 32, 143–165.
- Davis, B.A.S., Brewer, S., Stevenson, A.C., Guiot, J., 2003. The temperature of Europe during the Holocene reconstructed from pollen data. *Quat. Sci. Rev.* 22, 1701–1716.
- Davis, B.A.S., Zanon, M., Collins, P., Mauri, A., Bakker, J., Barboni, D., Barthelmes, A., Beaudouin, C., Birks, H.J.B., Bjune, A.E., Bradshaw, R., Brugia, E., Bunting, J., Connor, S., de Beaulieu, J.-L., Edwards, K., Ejarque, A., Fall, P., Florenzano, A., Fyfe, R., Galop, D., Giardini, M., Giesecke, T., Grant, M.J., Jahns, S., Jankowska, V., Juggin, S., Karmann, M., Karpinska-Kolaczek, M., Kolaczek, P., Kühl, N., Kunes, P., Lapteva, E.G., Leroy, S., Leydet, M., Lopez Saez, J.A., Maizier, F., Matthias, I., Meltssov, V., Mercuri, A.M., Miras, Y., Mitchell, F., Molinari, M., Morris, J., Naughton, F., Nielsen, A.B., Novenko, E., Odgaard, B., Ortú, E., Overballe-Petersen, M., Pardoe, H., Peglar, S.M., Pelanova, B., Pidek, I., Sadori, L., Seppä, H., Severova, E., Shaw, H., Swieta-Musznicka, J., Theuerkauf, M., Tonkov, S., Veski, S., van der Knaap, W.O., van Leeuwen, J., Vermeere, M., Woodbridge, J., Zimny, M., Kaplan, J., 2013. The European Modern Pollen Database (EMPD) project. *Veg. Hist. Archaeobot.* 22 (6), 521–530.
- Di Domenico, F., Lucchese, F., Magri, D., 2013. Buxus in Europe: Late Quaternary dynamics and modern vulnerability. *Perspect. Plant Ecol.* 14, 354–362.
- Enghoff, I.B., MacKenzie, B.R., Nielsen, E.E., 2007. The Danish fish fauna during the warm Atlantic period (ca. 7000–3900 BC): forerunner of future changes? *Fish. Res.* 87, 167–180.
- Finsinger, W., Heiri, O., Valsecchi, V., Tinner, W., Lotter, A.F., 2007. Modern pollen assemblages as climate indicators in southern Europe. *Glob. Ecol. Biogeogr.* 16, 567–582.
- Fischer, N., Jungclaus, J.H., 2011. Evolution of the seasonal temperature cycle in a transient Holocene simulation: orbital forcing and sea-ice. *Clim. Past* 7, 1139–1148.
- Fohlmeister, J., Schroder-Ritzrau, A., Scholz, D., Spotl, C., Riechelmann, D.F.C., Mudelsee, M., Wackerbarth, A., Gerdes, A., Riechelmann, S., Immenhauser, A., Richter, D.K., Mangini, A., 2012. Bunker Cave stalagmites: an archive for central European Holocene climate variability. *Clim. Past* 8, 1751–1764.
- Furrer, R., Nychka, D., Sain, S., 2010. Tools for Spatial Data. Package ‘Fields’. CRAN.
- Gaffney, V., Fitch, S., Smith, D., 2009. Europe's Lost World: the Rediscovery of Doggerland. Council for British Archaeology.
- Garzon, M.B., de Dios, R.S., Ollero, H.S., 2007. Predictive modelling of tree species distributions on the Iberian Peninsula during the Last Glacial Maximum and Mid-Holocene. *Ecography* 30, 120–134.
- Giesecke, T., Bjune, A.E., Chiverrell, R.C., Seppe, H., Ojala, A.E.K., Birks, H.J.B., 2008. Exploring Holocene continentality changes in Fennoscandia using present and past tree distributions. *Quat. Sci. Rev.* 27, 1296–1308.
- Giesecke, T., Hickler, T., Kunkel, T., Sykes, M.T., Bradshaw, R.H.W., 2007. Towards an understanding of the Holocene distribution of *Fagus sylvatica* L. *J. Biogeogr.* 34, 118–131.
- Giesecke, T., Davis, B., Brewer, S., Finsinger, W., Wolters, S., Blaauw, M., de Beaulieu, J.L., Binney, H., Fyfe, R.M., Gaillard, M.J., Gil-Romera, G., van der Knaap, W.O., Kunes, P., Kuhl, N., van Leeuwen, J.F.N., Leydet, M., Lotter, A.F., Ortú, E., Semmler, M., Bradshaw, R.H.W., 2014. Towards mapping the late Quaternary vegetation change of Europe. *Veg. Hist. Archaeobot.* 23, 75–86.
- Goehring, B.M., Schaefer, J.M., Schluechter, C., Lifton, N.A., Finkel, R.C., Jull, A.J.T., Akcar, N., Alley, R.B., 2011. The Rhone Glacier was smaller than today for most of the Holocene. *Geology* 39, 679–682.
- Grimm, E.C., Jacobson, G.L., 2004. Late-Quaternary vegetation history of the eastern United States. *Dev. Quat. Sci.* 1, 381–402.
- Gritti, E.S., Gachet, S., Sykes, M.T., Guiot, J., 2004. An extended probabilistic approach of plant vital attributes: an application to European pollen records at 0 and 6 ka. *Glob. Ecol. Biogeogr.* 13, 519–533.
- Grosjean, M., Suter, P.J., Trachsel, M., Wanner, H., 2007. Ice-borne prehistoric finds in the Swiss Alps reflect Holocene glacier fluctuations. *J. Quat. Sci.* 22, 203–207.
- Guiot, J., Harrison, S.P., Prentice, I.C., 1993. Reconstruction of Holocene precipitation patterns in Europe using pollen and lake-level data. *Quat. Res.* 40, 139–149.
- Gyllencreutz, R., Mangerud, J., Svendsen, J.I., Lohne, O., 2007. DATED – a GIS-based reconstruction and dating database of the Eurasian deglaciation. *Applied Quaternary Research in the Central Part of Glaciated Terrain. Geological Survey of Finland*, Special Paper 46, pp. 113–120.
- Hammarlund, D., Velle, G., Wolfe, B.B., Edwards, T.W.D., Barnekow, L., Bergman, J., Holmgren, S., Lamme, S., Snowball, I., Wohlfarth, B., Possnert, G., 2004. Palaeolimnological and sedimentary responses to Holocene forest retreat in the Scandes Mountains, west-central Sweden. *Holocene* 14, 862–876.
- Hargreaves, J.C., Annan, J.D., Ohgaito, R., Paul, A., Abe-Ouchi, A., 2013. Skill and reliability of climate model ensembles at the Last Glacial Maximum and mid-Holocene. *Clim. Past* 9, 811–823.
- Harrison, S., Prentice, C., 2003. Climate and CO<sub>2</sub> controls on global vegetation distribution at the last glacial maximum: analysis based on palaeovegetation data, biome modelling and palaeoclimate simulations. *Glob. Change Biol.* 9, 983–1004.
- Heiri, O., Lotter, A.F., Hausmann, S., Kienast, F., 2003. A chironomid-based Holocene summer air temperature reconstruction from the Swiss Alps. *Holocene* 13, 477–484.
- Hijmans, R.J., Cameron, S.E., Parra, J.L., Jones, P.G., Jarvis, A., 2005. Very high resolution interpolated climate surfaces for global land areas. *Int. J. Climatol.* 25, 1965–1978.
- Huntley, B., 1990a. European postglacial forests – compositional changes in response to climatic-change. *J. Veg. Sci.* 1, 507–518.
- Huntley, B., 1990b. Pollen-climate response surfaces and the study of climate change. In: Gray, J.M. (Ed.), *Proceedings of the QRA Discussion Meeting 329–356*, Manchester, pp. 73–106.
- Huntley, B., 1993. The use of climate response surfaces to reconstruct paleoclimate from Quaternary pollen and plant macrofossil data. *Philos. Trans. R. Soc. Lond. Ser. B-Biol. Sci.* 341, 215–223.
- Huntley, B., Birks, H.J.B., 1983. *An Atlas of Past and Present Pollen Maps for Europe: 0–13000 Years Ago*. Cambridge University Press, Cambridge.
- Huntley, B., Prentice, I.C., 1988. July temperatures in Europe from pollen data, 6000 years before present. *Science* 241, 687–690.
- Ilyashuk, E.A., Koinig, K.A., Heiri, O., Ilyashuk, B.P., Psenner, R., 2011. Holocene temperature variations at a high-altitude site in the Eastern Alps: a chironomid record from Schwarzsee ob Soden, Austria. *Quat. Sci. Rev.* 30, 176–191.
- Indermühle, A., Stocker, T.F., Joos, F., Fischer, H., Smith, H.J., Wahlen, M., Deck, B., Mastrioanni, D., Tschumi, J., Blunier, T., Meyer, R., Stauffer, B., 1999. Holocene carbon-cycle dynamics based on CO<sub>2</sub> trapped in ice at Taylor Dome, Antarctica. *Nature* 398, 121–126.
- Juggins, S., 2012. Rioja: Analysis of Quaternary Science Data. R package version (0.8–3).
- Juggins, S., 2013. Quantitative reconstructions in palaeolimnology: new paradigm or sick science? *Quat. Sci. Rev.* 64, 20–32.
- Juggins, S., Birks, H.J.B., 2011, 431–494. Quantitative environmental reconstructions from biological data. In: Birks, H.J.B., Lotter, A.F., Juggins, S., Smol, J.P. (Eds.), *Tracking Environmental Change Using Lake Sediments: Data Handling and Numerical Techniques*. Springer, pp. 431–494. ISBN: 978-94-007-2744-1.
- Kakroodi, A.A., Kroonenberg, S.B., Hoogendoorn, R.M., Khani, H.M., Yamani, M., Ghassemi, M.R., Lahijani, H.A.K., 2012. Rapid Holocene sea-level changes along the Iranian Caspian coast. *Quat. Int.* 263, 93–103.
- Kaplan, J.O., Krumhardt, K.M., Zimmermann, N., 2009. The prehistoric and pre-industrial deforestation of Europe. *Quat. Sci. Rev.* 28, 3016–3034.
- Kaplan, J.O., Krumhardt, K.M., Ellie, E.C., Ruddiman, W.F., Lemmen, C., Goldeijk, K.K., 2011. Holocene carbon emissions as a result of anthropogenic land cover change, 21 (5), 775–791.
- Kotthoff, U., Pross, J., Müller, U.C., Peyron, O., Schmidl, G., Schulz, H., Bordon, A., 2008. Climate dynamics in the borderlands of the Aegean Sea during formation of sapropel S1 deduced from a marine pollen record. *Quat. Sci. Rev.* 27, 832–845.
- Kuhl, N., Litt, T., 2003. Quantitative time series reconstruction of Eemian temperature at three European sites using pollen data. *Veg. Hist. Archaeobot.* 12, 205–214.
- Kuhl, N., Litt, T., Scholzel, C., Hense, A., 2007. Eemian and Early Weichselian temperature and precipitation variability in northern Germany. *Quat. Sci. Rev.* 26, 3311–3317.
- Lachniet, M.S., 2009. Climatic and environmental controls on speleothem oxygen-isotope values. *Quat. Sci. Rev.* 28, 412–432.
- Langdon, P.G., Barber, K.E., Lomas-Clarke, S.H., 2004. Reconstructing climate and environmental change in northern England through chironomid and pollen analyses: evidence from Talkin Tarn, Cumbria. *J. Paleolimnol.* 32, 197–213.
- Larocque-Tobler, I., Heiri, O., Wehrli, M., 2010. Late Glacial and Holocene temperature changes at Egelsee, Switzerland, reconstructed using subfossil chironomids. *J. Paleolimnol.* 43, 649–666.

- Leemans, R., Cramer, W.P., 1991. The IIASA Database for Mean Monthly Values of Temperature, Precipitation and Cloudiness of a Global Terrestrial Grid. International Institute of Applied Systems Analyses, Laxenburg, Austria.
- Lemmen, C., Wirtz, K.W., 2012. On the sensitivity of the simulated European Neolithic transition to climate extremes. *J. Archaeol. Sci.* 51, 65–72.
- Liu, Z., Otto-Bliesner, B., Clark, P., 2011. Synthesis of transient climate evolution of the last 21 ka (SynTReCE-21) workshop. *PAGES News* 19, 79–80.
- Lohmann, G., Lorenz, S.J., 2007. Orbital forcing on atmospheric dynamics during the last interglacial and glacial inception. In: Frank Sirocko, M.C.M.F.S.G., Thomas, L. (Eds.), *Developments in Quaternary Sciences*. Elsevier, pp. 527–545.
- Lorenz, S.J., Kim, J.H., Rimbu, N., Schneider, R.R., Lohmann, G., 2006. Orbitally driven insolation forcing on Holocene climate trends: evidence from alkenone data and climate modeling. *Paleoceanography* 21, Pa1002.
- Luetscher, M., Hoffmann, D.L., Frisia, S., Spotl, C., 2011. Holocene glacier history from alpine speleothems, Milchbach cave, Switzerland. *Earth Planet Sci. Lett.* 302, 95–106.
- Luterbacher, J., Garcia Herrera, R., Allan, R., Alvarez-Castro, B.G., Benito, G., Booth, J., Buntgen, U., Colombaroli, D., Davis, B., Esper, J., Felis, T., Fleitmann, D., Frank, D., Gallego, D., Gonzalez-Rouco, F.J., Goosse, H., Kiefer, T., Macklin, M.G., Montagna, P., Newman, L., Ribera, P., Roberts, N., Silenzi, S., Tinner, W., Valero-Garcés, B., van der Schrier, G., Vannière, B., Wanner, H., Werner, J.P., Willett, G., Xoplaki, C.S., Zerefos, E., Zorita, E., 2012. A review of 2000 years of paleoclimate evidence in the Mediterranean. In: Lionello, P. (Ed.), *The Climate of the Mediterranean Region: from the Past to the Future*. Elsevier Insights. Elsevier, Amsterdam, ISBN 9780124160422, pp. 87–186.
- Masson, V., Cheddadi, R., Braconnot, P., Joussaume, S., Texier, D., PMIP, 1999. Mid-Holocene climate in Europe: what can we infer from PMIP model data comparisons? *Clim. Dyn.* 15, 163–182.
- Mauri, A., Davis, B.A.S., Collins, P.M., Kaplan, J.O., 2014. The influence of atmospheric circulation on the mid-Holocene climate of Europe: a data-model comparison. *Clim. Past* 10, 1925–1938.
- Monnin, E., Indermühle, A., Dallenbach, A., Fluckiger, J., Stauffer, B., Stocker, T.F., Raynaud, D., Barnola, J.M., 2001. Atmospheric CO<sub>2</sub> concentrations over the last glacial termination. *Science* 291, 112–114.
- Nakagawa, T., Okuda, M., Yonenobu, H., Miyoshi, N., Fujiki, T., Gotanda, K., Tarasov, P.E., Morita, Y., Takemura, K., Horie, S., 2008. Regulation of the monsoon climate by two different orbital rhythms and forcing mechanisms. *Geology* 36, 491–494.
- Nesje, A., Kvamme, M., 1991. Holocene glacier and climate variations in western Norway – evidence for early Holocene glacier demise and multiple Neoglacial events. *Geology* 19, 610–612.
- Nicolussi, K., Kaufmann, M., Patzelt, G., van der Plicht, J., Thurner, A., 2005. Holocene tree-line variability in the Kauner Valley, Central Eastern Alps, indicated by dendrochronological analysis of living trees and subfossil logs. *Veg. Hist. Archaeobot.* 14, 221–234.
- Orland, I.J., Bar-Matthews, M., Ayalon, A., Matthews, A., Kozdon, R., Ushikubo, T., Valley, J.W., 2012. Seasonal resolution of Eastern Mediterranean climate change since 34 ka from a Soreq Cave speleothem. *Geochim. Cosmochim. Acta* 89, 240–255.
- Overpeck, J.T., Webb, T., Prentice, I.C., 1985. Quantitative interpretation of fossil pollen Spectra – dissimilarity coefficients and the method of modern analogs. *Quat. Res.* 23, 87–108.
- Peltier, W.R., 2004. Global glacial isostasy and the surface of the ice-age earth: the ice-5G (VM2) model and grace. *Annu. Rev. Earth. Planet. Sci.* 32, 111–149.
- Peltier, W.R., 2009. Closure of the budget of global sea level rise over the GRACE era: the importance and magnitudes of the required corrections for global glacial isostatic adjustment. *Quat. Sci. Rev.* 28, 1658–1674.
- Penalba, M.C., Arnold, M., Guiot, J., Duplessy, J.C., deBeaulieu, J.L., 1997. Termination of the last glaciation in the Iberian Peninsula inferred from the pollen sequence of Quintanar de la Sierra. *Quat. Res.* 48, 205–214.
- Peyron, O., Goring, S., Dormoy, I., Kotthoff, U., Pross, J., de Beaulieu, J.L., Drescher-Schneider, R., Vannière, B., Magny, M., 2011. Holocene seasonality changes in the central Mediterranean region reconstructed from the pollen sequences of Lake Accesa (Italy) and Tenaghi Philippon (Greece). *Holocene* 21, 131–146.
- Peyron, O., Guiot, J., Cheddadi, R., Tarasov, P., Reille, M., de Beaulieu, J.L., Bottema, S., Andrieu, V., 1998. Climatic reconstruction in Europe for 18,000 yr B.P. from pollen data. *Quat. Res.* 49, 183–196.
- Pla, S., Catalan, J., 2005. Chrysophyte cysts from lake sediments reveal the sub-millennial winter/spring climate variability in the northwestern Mediterranean region throughout the Holocene. *Clim. Dyn.* 24, 263–278.
- Prentice, I.C., Harrison, S.P., Jolly, D., Guiot, J., 1998. The climate and biomes of Europe at 6000 yr BP: comparison of model simulations and pollen-based reconstructions. *Quat. Sci. Rev.* 17, 659–668.
- Renssen, H., Goosse, H., Fichefet, T., Brovkin, V., Driesschaert, E., Wolk, F., 2005. Simulating the Holocene climate evolution at northern high latitudes using a coupled atmosphere-sea ice-ocean-vegetation model. *Clim. Dyn.* 24, 23–43.
- Renssen, H., Seppä, H., Crosta, X., Goosse, H., Roche, D.M., 2012. Global characterization of the Holocene Thermal Maximum. *Quat. Sci. Rev.* 48, 7–19.
- Renssen, H., Seppä, H., Heiri, O., Roche, D.M., Goosse, H., Fichefet, T., 2009. The spatial and temporal complexity of the Holocene thermal maximum. *Nat. Geosci.* 2, 410–413.
- Saltre, F., Saint-Amant, R., Gritti, E.S., Brewer, S., Gaucherel, C., Davis, B.A.S., Chuine, I., 2013. Climate or dispersal: what limited European beech postglacial colonization. *Glob. Ecol. Biogeogr.* 22, 1217–1227.
- Sawada, M., Viau, A.E., Vettoretti, G., Peltier, W.R., Gajewski, K., 2004. Comparison of North-American pollen-based temperature and global lake-status with CCCma AGCM2 output at 6 ka. *Quat. Sci. Rev.* 23, 225–244.
- Seppä, H., Bennett, K.D., 2003. Quaternary pollen analysis: recent progress in palaeoecology and palaeoclimatology. *Prog. Phys. Geogr.* 27, 548–579.
- Seppä, H., Bjune, A.E., Telford, R.J., Birks, H.J.B., Veski, S., 2009. Last nine-thousand years of temperature variability in Northern Europe. *Clim. Past* 5, 523–535.
- Singarayer, J.S., Valdes, P.J., Friedlingstein, P., Nelson, S., Beerling, D.J., 2011. Late Holocene methane rise caused by orbitally controlled increase in tropical sources. *Nature* 470, 82–U91.
- Sundqvist, H.S., Zhang, Q., Moberg, A., Holmgren, K., Kornich, H., Nilsson, J., Brattstrom, G., 2010. Climate change between the mid and late Holocene in northern high latitudes – part 1: survey of temperature and precipitation proxy data. *Clim. Past* 6, 591–608.
- Terral, J., Arnold-Simard, G., 1996. Beginnings of olive cultivation in eastern Spain in relation to Holocene bioclimatic changes. *Quat. Res.* 46, 176–185.
- Turney, C., Baillie, M., Clemens, S., Brown, D., Palmer, J., Pilcher, J., Reimer, P., Leuschner, H.H., 2005. Testing solar forcing of pervasive Holocene climate cycles. *J. Quat. Sci.* 20, 511–518.
- Velle, G., Brodersen, K.P., Birks, H.J.B., Willlassen, E., 2010. Midges as quantitative temperature indicator species: lessons for palaeoecology. *Holocene* 20, 989–1002.
- Velle, G., Brooks, S.J., Birks, H.J.B., Willassen, E., 2005. Chironomids as a tool for inferring Holocene climate: an assessment based on six sites in southern Scandinavia. *Quat. Sci. Rev.* 24, 1429–1462.
- Verheyden, S., Nader, F.H., Cheng, H.J., Edwards, L.R., Swennen, R., 2008. Paleoclimate reconstruction in the Levant region from the geochemistry of a Holocene stalagmite from the Jeita cave, Lebanon. *Quat. Res.* 70, 368–381.
- von Grafenstein, U., Erlenkeuser, H., Brauer, A., Jouzel, J., Johnsen, S.J., 1999. A mid-European decadal isotope-climate record from 15,500 to 5000 years BP. *Science* 284, 1654–1657.
- Vork, K.A., Thomsen, E., 1996. Lusitanian/Mediterranean ostracods in the Holocene of Denmark: implications for the interpretation of winter temperatures during the postglacial temperature maximum. *Holocene* 6, 423–432.
- Wohlfahrt, J., Harrison, S.P., Braconnot, P., 2004. Synergistic feedbacks between ocean and vegetation on mid- and high-latitude climates during the mid-Holocene. *Clim. Dyn.* 22, 223–238.
- Woillez, M.N., Kageyama, M., Krinner, G., de Noblet-Ducoudre, N., Viovy, N., Mancip, M., 2011. Impact of CO<sub>2</sub> and climate on the Last Glacial Maximum vegetation: results from the ORCHIDEE/IPSL models. *Clim. Past* 7, 557–577.
- Wu, H.B., Guiot, J.L., Brewer, S., Guo, Z.T., 2007. Climatic changes in Eurasia and Africa at the last glacial maximum and mid-Holocene: reconstruction from pollen data using inverse vegetation modelling. *Clim. Dyn.* 29, 211–229.
- Zhang, Q., Sundqvist, H.S., Moberg, A., Kornich, H., Nilsson, J., Holmgren, K., 2010. Climate change between the mid and late Holocene in northern high latitudes – part 2: model-data comparisons. *Clim. Past* 6, 609–626.